# Convergence of Bi-Virus Epidemic Models With Non-Linear Rates on Networks—A Monotone Dynamical Systems Approach

Vishwaraj Doshi<sup>®</sup>, Shailaja Mallick<sup>®</sup>, and Do Young Eun<sup>®</sup>, Senior Member, IEEE

Abstract—We study convergence properties of competing epidemic models of the Susceptible-Infected-Susceptible (SIS) type. The SIS epidemic model has seen widespread popularity in modelling the spreading dynamics of contagions such as viruses, infectious diseases, or even rumors/opinions over contact networks (graphs). We analyze the case of two such viruses spreading on overlaid graphs, with non-linear rates of infection spread and recovery. We call this the *non-linear bi-virus model* and, building upon recent results, obtain precise conditions for global convergence of the solutions to a trichotomy of possible outcomes: a virus-free state, a single-virus state, and to a coexistence state. Our techniques are based on the theory of monotone dynamical systems (MDS), in contrast to Lyapunov based techniques that have only seen partial success in determining convergence properties in the setting of competing epidemics. We demonstrate how the existing works have been unsuccessful in characterizing a large subset of the model parameter space for bi-virus epidemics, including all scenarios leading to coexistence of the epidemics. To the best of our knowledge, our results are the first in providing complete convergence analysis for the bi-virus system with nonlinear infection and recovery rates on general graphs.

*Index Terms*—Epidemics on networks, bi-virus models, multi-layer graphs, monotone dynamical systems.

#### I. INTRODUCTION AND OVERVIEW

RAPH-BASED epidemic models are widely employed to analyze the spread of real world phenomena such as communicable diseases [2], [3], computer viruses, malware [4], [5], [6], product adoption [7], [8], [9], opinions, and rumors [10], [11], [12], [13]. The propagation of such phenomenon (which we cumulatively refer to as *epidemics* or *viruses*)

Manuscript received 28 July 2021; revised 7 March 2022 and 29 July 2022; accepted 23 September 2022; approved by IEEE/ACM TRANSACTIONS ON NETWORKING Editor J. Ghaderi. Date of publication 18 October 2022; date of current version 16 June 2023. This work was supported in part by the National Science Foundation under Grant CNS-2007423 and Grant CNS-1824518. A subset of the material in this paper appears in [DOI: 10.1109/INFOCOM42981.2021.9488828]. (Corresponding author: Do Young Eun.)

Vishwaraj Doshi was with the Operations Research Graduate Program, North Carolina State University, Raleigh, NC 27695 USA. He is now with the Data Science and Advanced Analytics, IQVIA Inc., Plymouth Meeting, PA 19462 USA (e-mail: vdoshi@ncsu.edu).

Shailaja Mallick is with the Department of Computer Science, North Carolina State University, Raleigh, NC 27695 USA (e-mail: smallic@ncsu.edu).

Do Young Eun is with the Department of Electrical and Computer Engineering, North Carolina State University, Raleigh, NC 27695 USA (e-mail: dyeun@ncsu.edu).

This article has supplementary downloadable material available at https://doi.org/10.1109/TNET.2022.3213015, provided by the authors.

Digital Object Identifier 10.1109/TNET.2022.3213015

usually takes place via processes such as human contact, word-of-mouth, exchange of emails or even in social media platforms. Graph based techniques, with edge based mechanisms to model information spread, have therefore proven to be effective in capturing such epidemic dynamics, and have been a research focus over the past few decades [14], [15], [16], [17]. In recent years, the development of models which capture the competition of two or more of such epidemics has seen a surge of interest. In particular, models capturing the behavior of *two competing* epidemics of the *Susceptible-Infected-Susceptible* (SIS) types, also known as the *bi-virus* or *bi-SIS* models, have garnered significant attention over the years [8], [18], [19], [20], [21].

Epidemic models take the form of ordinary differential equations (ODEs) and their analysis involves the identification of fixed points of the system, their uniqueness properties, and ultimately showing the convergence of the solution trajectories to those fixed points. The technique via Lyapunov functions has historically been a popular method to prove convergence to fixed points and was also used in epidemiology literature to derive the convergence properties of the SIS epidemic model. The SIS model was originally introduced in [2] to capture the spread of Gonorrhea due to contact between individuals in a population, and was further developed in [22], [23], [24], [25], [26], [27], [28], and [29]. The central result for SIS epidemics, originally proved using Lyapunov functions in [2], is a *dichotomy* arising from the relation between model parameter  $(\tau > 0)$  representing the effective infection rate or strength of the virus, and a threshold value ( $\tau^* > 0$ ). When  $\tau \leq \tau^*$ , the virus spread is not strong enough and the system converges to a 'virus-free' state. When  $\tau > \tau^*$ , it converges to a state where the virus infects a non-zero portion of the population. Attempts have also been made to perform similar convergence analysis for the bi-virus epidemic model [8], [19], [20], [21]. The key questions posed in such literature are: Can both competing epidemics coexist over the network? If not, which one prevails? Or do both die out? This trichotomy of possible results is what the recent literature has been trying to characterize.

When the propagation of the two epidemics occurs over the same network [8], [30], it has been established that coexistence of two viruses is impossible except in the

 $<sup>^{1}\</sup>tau = \beta/\delta$ , where  $\beta > 0$  stands for the infection rate of the virus and  $\delta > 0$  the recovery rate from the virus. Section II provides a detailed explanation.

rare cases where their effective strengths  $(\tau_1, \tau_2 > 0)$  for viruses 1, 2, respectively) are equal [8], [18], [19], [20], [21]; the virus with the larger effective strength otherwise wiping out the other, a phenomenon sometimes referred to as winner takes all [8]. The situation is much more complicated when the two viruses spread over two distinct networks overlaid on the same set of nodes. This modeling approach is more representative of the real world, where competing rumors/products/memes may not use the same platforms to propagate, though they target the same individuals. Recent works [18], [19], [20], [21], [31], [32], [33], [34] therefore consider this more general setting, but unfortunately, a complete characterization of the trichotomy of outcomes has still proven to be elusive and remains open as of now.

While the original SIS model introduced in [2] had the aggregate infection and recovery rates of a node as linear functions of the number of infected neighbors, there has been a push towards studying more generalized models where these rates are made heterogeneous (across nodes) and nonlinear [35], [36], [37], [38], [39]. Realistic assumptions such as infection rates tending to saturation with continual increase in neighborhood infection [40], [41], [42], [43] have become more commonplace, implying that the models employing strictly linear spreading dynamics often provide overestimates to the real world infection rates [20], [24]. This paper does not concern itself with answering which non-linear infection rate best captures the exact dynamics, but we direct the readers to [20] which provides simulation results comparing non-linear rate functions to the exact Markovian dynamics for some special randomly generated graph topologies. In some special cases, non-linear recovery rates also have an interpretation linking them to reliability theory in the form infection duration with increasing failure rates (failure here being the recovery of an infected node). Allowing for non-linear infection and recovery rates leads to a more general version of the bi-virus model on overlaid graphs, albeit much more complicated, and the complete convergence criterion is yet to be fully established [19], [20]. It should be noted that while we extensively refer to the infection and recovery rates being either linear or non-linear in this paper, the bi-virus epidemic model itself will always be a system of non-linear ODEs.

**Limitations of existing works** Of all the recent works concerning the spread of SIS type bi-virus epidemics on overlaid networks, [20] and [19] provide conditions under which the system globally converges to the state where one virus survives while the other dies out. [20] approaches the problem of showing global convergence by employing the classic technique via Lyapunov functions. However, finding appropriate Lyapunov functions is a highly non-trivial task, and as mentioned in [19], is even more difficult due to the coupled nature of the bi-virus ODE system. This can be seen in the condition they derive in [20] for the case where, say, Virus 1 dies out and Virus 2 survives. When  $\tau_1$  and  $\tau_2$  represent the effective strengths of Virus 1 and Virus 2, respectively, their condition translates to  $\tau_1 \leq \tau_1^*$  where  $\tau_1^*$  is the threshold corresponding to the single-virus case, meaning that Virus 1 would not have survived even if it was the only epidemic

present on the network. More importantly, [20] is unable to characterize convergence properties for  $\tau_1 > \tau_1^*$  and  $\tau_2 > \tau_2^*$ .

The authors in [19] take a different approach and tackle this problem by applying their 'qualitative analysis' technique, which uses results from other dynamical systems that bound the solutions of the bi-virus ODE; and provide conditions under which the system globally converges to single-virus equilibria. As we show later in Section V-B, however, their conditions not only characterize just a *subset* of the actual space of parameters that lead to global convergence to the single-virus equilibria (which they themselves pointed out), but the size of this subset is highly sensitive to the graph topology, often much smaller than what it should be in general. In other words, a complete characterization of the *entire* space of model parameters, on which the system globally converges to one of the trichotomic states, has still been recognized as an open problem in the bi-virus literature [19], [20], [21].

*Our contributions* In this paper, we analyze the bi-virus model with non-linear infection and recovery rates (or the non-linear bi-virus model in short) and provide the complete characterization of the trichotomy of the outcomes with necessary and sufficient conditions under which the system globally converges to one of the three possible points: (i) a 'virus-free' state, (ii) a 'single-virus' equilibrium, or (iii) an equilibrium where both viruses coexist over the network. While the result for convergence to the virus-free state of the bi-SIS model is not new for non-linear infection and linear recovery rates, our proof for the same is the most general form known to date, covering the case with both infection and recovery rates being non-linear. The proof of convergence to the virus-free state of the bi-virus model is straightforward, and directly follows from the convergence criterion for the single-virus SIS model with non-linear rates. However, the convergence results for fixed points where only one of the two viruses survives, or to the equilibrium where both viruses coexist, are not as straightforward to establish, rendering the typical Lyapunov based approach largely inapplicable.

In proving these results, we first show, using a specially constructed cone based partial ordering, that the bi-virus epidemic model possesses some inherent monotonicity properties. We then use novel techniques from the theory of *monotone* dynamical systems (MDS) [44] to prove our main results. In recent control systems literature [45], [46], [47], [48], [49], techniques based on the construction of cone based partial orderings that leverage the monotonicity properties of dynamical systems have indeed been studied. Dynamical systems exhibiting such monotonicity properties are also sometimes called deferentially positive systems [50] and cooperative systems [51] in the ODE setting, with interesting applications in consensus problems for distributed systems [52] and even neural networks [53]. In this paper, we utilize these MDS techniques in the setting of competing epidemics, and as a result demonstrate an alternative to Lyapunov based approaches to analyze convergence properties of epidemic models. The novelty of using the MDS approach for analysis also lies with [54], which uses similar techniques to analyze the bi-virus system for the special case of linear infection and recovery rates, and was developed concurrently and independently with

the initial version of this work [1]. This further highlights the utility of MDS techniques for the analysis of epidemic models on graphs.

This paper is an extension of our previous work [1], which gives necessary and sufficient conditions for convergence to the three types of equilibria only for the special case of the bi-virus model with *linear* infection and recovery rates (or the linear bi-virus model in short). Our conditions therein take a more precise form in terms of the model parameters  $au_1$  and  $au_2$  and one can visualize an exact partition of the model parameter space into regions corresponding to various convergence outcomes. We note that this partition of the model parameter space coincides with that in [18], wherein they employed only *local* stability results via bifurcation analysis - concerning only solution trajectories that originate from a small neighborhood of those fixed points. In contrast, our results in this paper concern global stability of the system with any combination of linear as well as more general, non-linear infection and recovery rates.

Structure of the paper In Section II, we first introduce the basic notation used throughout the paper, along with the classical (single-virus) SIS model and the bi-virus model. We then provide the generalization to non-linear infection and recovery rates in Section III with some key assumptions on the infection and recovery rate functions, complimented by a discussion in Appendix A regarding a special class of recovery rates. In Section IV, we provide a primer to the MDS theory, and establish monotonicity results for the single-virus SIS model, proving the convergence result for the single-virus model with non-linear infection and recovery rates whose proofs are deferred to Appendix C. We then go on to show in Section V-A that the non-linear bi-virus model is also a monotone dynamical system with respect to a specially constructed cone-based partial ordering, and include the main convergence results in Section V-B. In Section VI we take the opportunity to provide a more intuitive version of our results by considering the special case of linear infection and recovery rates, along with brief comparisons with the existing literature. In Section VII, we provide numerical results which confirm our theoretical findings. We then conclude in Section VIII.

We include additional Appendices for our paper as supplementary material [55]. For better readability of the paper, all technical proofs of the main results are deferred to Appendix F in [55]. The appendices also include some selected definitions and results from matrix theory (Appendix D), ODE theory (Appendix E), and from MDS theory (Appendix B), which we use as part of our proofs of the Theorems in Section V-B.

## II. PRELIMINARIES

#### A. Basic Notations

We standardize the notations of vectors and matrices by using lower case, bold-faced letters to denote vectors ( $\mathbf{v} \in \mathbb{R}^N$ ), and upper case, bold-faced letters to denote matrices ( $\mathbf{M} \in \mathbb{R}^{N \times N}$ ). We denote by  $\lambda(\mathbf{M})$  the largest *real part*<sup>2</sup> of

all eigenvalues of a square matrix M. We use  $\operatorname{diag}(\mathbf{v})$  or  $\mathbf{D}_{\mathbf{v}}$ to denote the  $N \times N$  diagonal matrix with entries of vector  $\mathbf{v} \in \mathbb{R}^N$  on the diagonal. Also, we denote  $\mathbf{1} \triangleq [1, \cdots, 1]^T$ and  $\mathbf{0} \triangleq [0, \dots, 0]^T$ , the N-dimensional vector of all ones and zeros, respectively. For vectors, we write  $\mathbf{x} \leq \mathbf{y}$  to indicate that  $x_i \le y_i$  for all i;  $\mathbf{x} < \mathbf{y}$  if  $\mathbf{x} \le \mathbf{y}$  and  $\mathbf{x} \ne \mathbf{y}$ ;  $\mathbf{x} \ll \mathbf{y}$  when all entries satisfy  $x_i < y_i$ . We use  $\mathcal{G}(\mathcal{N}, \mathcal{E})$  to represent a general, undirected, connected graph with  $\mathcal{N} \triangleq \{1, 2, \dots, N\}$  being the set of nodes and  $\mathcal E$  being the set of edges. When we refer to a matrix  $\mathbf{A} = [a_{ij}]$  as the adjacency matrix of some graph  $\mathcal{G}(\mathcal{N}, \mathcal{E})$ , it satisfies  $a_{ij} \triangleq \mathbb{1}_{\{(i,j)\in\mathcal{E}\}}$  for any  $i, j \in \mathcal{N}$ ; we use  $d_{min}(\mathbf{A})$  and  $d_{max}(\mathbf{A})$  to denote the minimum and maximum degrees of the nodes of the corresponding graph. Since we only consider connected graphs, all the adjacency matrices in this paper are automatically considered to be irreducible (see Definition D.1 in Appendix D).

#### B. SIS Model With Linear Rates

Consider the graph  $\mathcal{G}(\mathcal{N}, \mathcal{E})$ , and assume that at any given time  $t \geq 0$ , each node  $i \in \mathcal{N}$  of the graph is either in an infected (I), or in a susceptible (S) state. An infected node can infect each of its susceptible neighbors with rate  $\beta > 0$ . It can also, with rate  $\delta > 0$ , be cured from its infection and revert to being susceptible again. We write  $\mathbf{x}(t) = [x_i(t)] \in \mathbb{R}^N$ , where  $x_i(t)$  represents the probability that node  $i \in \mathcal{N}$  is infected at any given time  $t \geq 0$ . Then, the dynamics of the SIS model can be captured via the system of ODEs given by

$$\frac{dx_i(t)}{dt} \triangleq \beta(1 - x_i(t)) \sum_{j \in \mathcal{N}} a_{ij} x_j(t) - \delta x_i(t)$$
 (1)

for all  $i \in \mathcal{N}$  and  $t \ge 0$ . In a matrix-vector form, this can be written as

$$\frac{d\mathbf{x}}{dt} \triangleq \beta \operatorname{diag}(\mathbf{1} - \mathbf{x})\mathbf{A}\mathbf{x} - \delta\mathbf{x} \tag{2}$$

where we suppress the (t) notation for brevity. The system (2) is positively invariant in the set  $[0,1]^N$ , and has  $\mathbf{0}$  as a fixed point (the virus-free equilibrium). The following result is well known from [2], which we will generalize in Section IV-B.

Theorem 2.1 (Theorem 3.1 in [2]): Let  $\tau \triangleq \beta/\delta$ . Then,

- (i) either  $\tau \leq 1/\lambda(\mathbf{A})$ , and  $\mathbf{x}^* = \mathbf{0}$  is a globally asymptotically stable fixed point of (2);
- (ii) or  $\tau > 1/\lambda(\mathbf{A})$ , and there exists a unique, strictly positive fixed point  $\mathbf{x}^* \in (0,1)^N$  such that  $\mathbf{x}^*$  is globally asymptotically stable in  $[0,1]^N \setminus \{0\}$ .

# C. Bi-Virus Model With Linear Rates

Consider two graphs  $\mathcal{G}_1(\mathcal{N}, \mathcal{E}_1)$  and  $\mathcal{G}_2(\mathcal{N}, \mathcal{E}_2)$ , on the same set of nodes  $\mathcal{N}$  but with different edge sets  $\mathcal{E}_1$  and  $\mathcal{E}_2$ . At any given time  $t \geq 0$ , a node  $i \in \mathcal{N}$  is either *infected by Virus* I, *infected by Virus* I, or is *susceptible*. A node infected by Virus 1 infects each of its susceptible neighbors with rate  $\beta_1 > 0$ , just like in the SIS model, but does so only to nodes which are its neighbors with respect to the graph  $\mathcal{G}_1(\mathcal{N}, \mathcal{E}_1)$ .

<sup>3</sup>We say an event occurs with some *rate*  $\alpha > 0$  if it occurs after a random amount of time, exponentially distributed with parameter  $\alpha > 0$ .

<sup>&</sup>lt;sup>2</sup>We use the  $\lambda$  notation instead of something like  $\lambda_{Re}$ , since it will mostly be used in cases where the largest eigenvalue is real, for which  $\lambda$  itself is the largest real eigenvalue. For example,  $\lambda(\mathbf{A})$  becomes the spectral radius for any non-negative matrix  $\mathbf{A}$  [56], [57].

Nodes infected by Virus 1 also recover with rate  $\delta_1 > 0$ , after which they enter the susceptible state. Similarly, nodes infected by Virus 2 infect their susceptible neighbors, this time with respect to the graph  $\mathcal{G}_2(\mathcal{N}, \mathcal{E}_2)$ , with rate  $\beta_2 > 0$ , while recovering with rate  $\delta_2 > 0$ . This competing bi-virus model of epidemic spread, also referred to as the  $SI_1I_2S$  model, can be represented by the following ODE system:

$$\frac{dx_i}{dt} \triangleq \beta_1 (1 - x_i - y_i) \sum_{j \in \mathcal{N}} a_{ij} x_j - \delta_1 x_i$$

$$\frac{dy_i}{dt} \triangleq \beta_2 (1 - x_i - y_i) \sum_{j \in \mathcal{N}} b_{ij} y_j - \delta_2 y_i \tag{3}$$

for all  $i \in \mathcal{N}$  and t > 0. In matrix-vector form, (3) becomes:

$$\frac{d\mathbf{x}}{dt} \triangleq \beta_1 \operatorname{diag} (\mathbf{1} - \mathbf{x} - \mathbf{y}) \, \mathbf{A} \mathbf{x} - \delta_1 \mathbf{x} 
\frac{d\mathbf{y}}{dt} \triangleq \beta_2 \operatorname{diag} (\mathbf{1} - \mathbf{x} - \mathbf{y}) \, \mathbf{B} \mathbf{y} - \delta_2 \mathbf{y}, \tag{4}$$

where  $\mathbf{A} = [a_{ij}]$  and  $\mathbf{B} = [b_{ij}]$  are the adjacency matrices of graphs  $\mathcal{G}_1(\mathcal{N}, \mathcal{E}_1)$  and  $\mathcal{G}_2(\mathcal{N}, \mathcal{E}_2)$ , respectively.

# III. EPIDEMIC MODELS WITH NON-LINEAR INFECTION AND RECOVERY RATES

In this section, we introduce the single-virus and bi-virus SIS models with non-linear infection and recovery rates. Nonlinearities can be attributed to the spread and recovery from the virus being related to the susceptibility of the disease (or its prevalence in the population) in a more complicated manner. This is more general than simply exponential random variables with constant rates used to model the spreading and recovery processes, which in aggregate scale linearly with the infection probabilities.<sup>4</sup> This is shown to be limiting in accurately modelling the trajectories of an infection spread; the linear scaling of the infection and recovery rates shown to being an overestimate to what is observed in reality [20], [37]. Many works thus argue for the modelling of these spreading processes with non-linear functions [35], [36], [38], [40]. We first present the more general single-virus SIS model with a set of intuitive assumptions (A1)-(A5) for the non-linear infection and recovery rates.

# A. SIS Model With Non-Linear Rates

In (1) the term  $\sum_{j\in\mathcal{N}} a_{ij}x_j(t)$  denotes the overall rate at which a susceptible node  $i\in\mathcal{N}$  gets infected by its neighbors. In what follows, we replace this by a generic function  $f_i(\mathbf{x}(t))$ , thereby allowing the overall infection rate for each node to be any non-linear function of  $x_i(t)$  for all neighbors j of i. Similarly, we replace the term  $\delta x_i(t)$ , denoting the overall recovery rate for any node  $i \in \mathcal{N}$ , by a non-linear function  $q_i(\mathbf{x}(t))$ . This generic version of the SIS model, allowing for non-linear infection and recovery rates, is given by the ODE

$$\frac{dx_i(t)}{dt} = \bar{f}_i(\mathbf{x}(t)) \triangleq (1 - x_i(t))f_i(\mathbf{x}(t)) - q_i(\mathbf{x}(t))$$
 (5)

for all  $i \in \mathcal{N}$  and  $t \geq 0$ . In a matrix-vector form, this can be written as

$$\frac{d\mathbf{x}}{dt} = \bar{F}(\mathbf{x}) \triangleq \operatorname{diag}(\mathbf{1} - \mathbf{x})F(\mathbf{x}) - Q(\mathbf{x})$$
 (6)

where  $F(\mathbf{x}) = [f_i(\mathbf{x})] \in \mathbb{R}^N$ , and  $Q(\mathbf{x}) = [q_i(\mathbf{x})] \in \mathbb{R}^N$  are the vectors of non-linear infection and recovery rate functions, respectively. We assume that they are continuous and twice differentiable in  $[0,1]^N$ , with  $\mathbf{J}_F(\mathbf{x})$  and  $\mathbf{J}_Q(\mathbf{x})$  denoting the Jacobians of F and Q respectively, evaluated at any point  $\mathbf{x} \in [0,1]^N$ . We now make the following key assumptions:

- (A1)  $F(\mathbf{0}) = \mathbf{0}$  and  $Q(\mathbf{0}) = \mathbf{0}$ ; (A2)  $[\mathbf{J}_F(\mathbf{x})]_{ij} = \frac{\partial f_i(\mathbf{x})}{\partial x_j} > 0 \quad \forall i \neq j \text{ with } a_{ij} > 0, \text{ otherwise}$   $[\mathbf{J}_F(\mathbf{x})]_{ij} = 0;$
- (A3)  $[\mathbf{J}_Q(\mathbf{x})]_{ii} = \frac{\partial q_i(\mathbf{x})}{\partial x_i} > 0$ , and  $[\mathbf{J}_Q(\mathbf{x})]_{ij} = \frac{\partial q_i(\mathbf{x})}{\partial x_j} \leq 0$  for all  $i \neq j$ ,  $\mathbf{x} \in [0,1]^N$ . Moreover,  $\sum_{i \neq j} [\mathbf{J}_Q(\mathbf{x})]_{ij} < 0$
- (A4)  $f_i(\mathbf{x})$  is concave in  $[0,1]^N$ , that is,  $\frac{\partial^2 f_i}{\partial x_i \partial x_k} \leq 0$  for all
- (A5)  $q_i(\mathbf{x})$  is convex function of  $x_i \in [0,1]^N$ , and a concave function of  $x_j$  for all  $j \neq i$ . That is,  $\frac{\partial^2 q_i}{\partial^2 x_i} \geq 0$  and  $\frac{\partial^2 q_i}{\partial x_i \partial x_k} \le 0$  for all  $i \in \mathcal{N}$ , and  $j, k \in \mathcal{N} \setminus \{i\}$ .

Assumption (A1) ensures that the virus-free state is a fixed point of (6), while (A2) is a proximity assumption that models infection spread only through edges of the underlying graph. Assumption (A3) concerns with the recovery rate, allowing it to be reduced by infected neighbors while still being nonegative. (A4) and (A5) assume concavity properties of the functions  $f_i(\mathbf{x})$  and  $g_i(\mathbf{x})$  in  $x_j$  for any neighbor j of i. This allows the effect of neighborhood infection  $x_j$  to saturate<sup>5</sup> as  $x_i$  increases. Assumption (A5) also assumes convexity of  $q_i(\mathbf{x})$  in local infection  $x_i$ , which means that increase in recovery rate caused by  $x_i$  can be larger as  $x_i$  increases.

Examples for non-linear infection rates satisfying (A1)–(A5) include logarithmic functions  $f_i(\mathbf{x})$  $\sum_{i} a_{ij} \ln (1+x_j)$ , similar to those in [20]. Examples of non-linear recovery rates include polynomial functions such as  $q_i(\mathbf{x}) = (1+x_i)^k - 1$  for any  $k \ge 1$ . A special class of the permissible non-linear recovery rates, where the infection duration is dependent solely on local infection  $x_i$ , is related to processes that have decreasing failure rates (DFR).<sup>6</sup> This special class of recovery processes that are DFR also includes the case of linear recovery rates. Note that our assumptions allow  $f_i(\mathbf{x})$  and  $q_i(\mathbf{x})$  to be heterogeneous

<sup>4&#</sup>x27;Aggregate' here refers to the mean field approximation which is one way to derive SIS-type ODEs. Another way is the large population mean field limit of a stochastic process, where the connection to the corresponding ODE system is formed via the Kurtz's theorem [16]. In this case, linearity is induced by the uniform or homogeneous mixing assumption which is also a subject of criticism in epidemiology literature [35], [36], [37], [38].

<sup>&</sup>lt;sup>5</sup>As  $x_j$  increases for any neighbor j of node i, the magnitude of the resulting change in both infection rate  $f_i(\mathbf{x})$  and recovery rate  $q_i(\mathbf{x})$  decreases. This is similar to the case of diminishing returns.

<sup>&</sup>lt;sup>6</sup>Failure rate for a non-negative random variable is defined as the ratio between its probability density function (PDF) and its complimentary cumulative distribution function (CCDF). In the context of infection duration, decreasing failure rate means that nodes recover at a decreased rate the longer they stay continuously infected. A more detailed discussion regarding the connection to SIS recovery rates can be found in Appendix A.

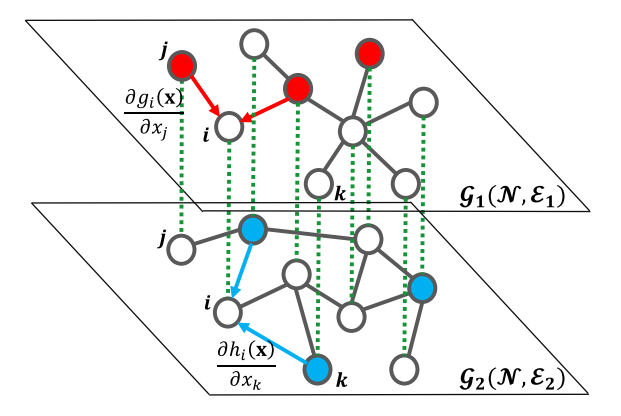


Fig. 1. Bi-Virus epidemic spread across overlaid graphs sharing the same set of nodes. Red and Blue arrows denote the spread of Virus 1 and 2, respectively from infected nodes j and k (coloured Red and Blue) to the susceptible node i (uncoloured) with the instantaneous rates as shown. The infected Red and Blue nodes also recover with a total rate of  $r_i(\mathbf{x})$  and  $s_i(\mathbf{y})$  for any node  $i \in \mathcal{N}$ , respectively.

across all nodes  $i \in \mathcal{N}$ , and the case with linear rates in (2) readily satisfies (A1)–(A5). This also extends to the linear bi-virus model (4) being a special case of the non-linear bi-virus model introduced in the next subsection, with infection and recovery rate functions therein satisfying the same assumptions (A1)–(A5).

#### B. Bi-Virus Model With Non-Linear Rates

The Bi-Virus model with non-linear infection and recovery rates is given by the following coupled system of ODEs:

$$\frac{dx_i}{dt} = \bar{g}_i(\mathbf{x}, \mathbf{y}) \triangleq (1 - x_i - y_i) g_i(\mathbf{x}(t)) - r_i(\mathbf{x})$$

$$\frac{dy_i}{dt} = \bar{h}_i(\mathbf{x}, \mathbf{y}) \triangleq (1 - x_i - y_i) h_i(\mathbf{y}(t)) - s_i(\mathbf{y}) \quad (7)$$

for all  $i \in \mathcal{N}$  and  $t \geq 0$ . In a matrix-vector form, (7) becomes:

$$\frac{d\mathbf{x}}{dt} = \bar{G}(\mathbf{x}, \mathbf{y}) \triangleq \operatorname{diag}(\mathbf{1} - \mathbf{x} - \mathbf{y}) G(\mathbf{x}) - R(\mathbf{x})$$

$$\frac{d\mathbf{y}}{dt} = \bar{H}(\mathbf{x}, \mathbf{y}) \triangleq \operatorname{diag}(\mathbf{1} - \mathbf{x} - \mathbf{y}) H(\mathbf{y}) - S(\mathbf{y}), \quad (8)$$

where  $G(\mathbf{x}) = [g_i(\mathbf{x})]$ ,  $R(\mathbf{x}) = [r_i(\mathbf{x})]$ , and  $H(\mathbf{y}) = [h_i(\mathbf{y})]$ ,  $S(\mathbf{y}) = [s_i(\mathbf{y})]$  are the non-linear infection and recovery rate functions for viruses 1 and 2, respectively. The pairs (G,R) and (H,S) each satisfy the assumptions (A1)–(A5); where G and H specifically satisfy (A2) with respect to their corresponding graphs with adjacency matrices  $\mathbf{A}$  and  $\mathbf{B}$ , respectively. Figure 1 illustrates of how these competing epidemics spread over the corresponding overlaid graphs.

Assumptions (A1)–(A5) are also more general (weaker) than those assumed in [19] and [20], where the recovery rates are restricted to being linear functions and are thus a special case of our model. We emphasize that while the set off assumptions for non-linear rates are mostly similar to (slightly more general than) those in literature, the characterization of all convergence scenarios for their respective bi-virus models is incomplete, as we shall discuss later in Section VI.

# IV. MONOTONE DYNAMICAL SYSTEMS AND THE SINGLE VIRUS EPIDEMIC

In this section, we provide a succinct introduction to monotone dynamical systems (MDS) and some important definitions therein. We go on to show that the SIS model (6) is a monotone dynamical system (specifically a cooperative system) and briefly apply these MDS techniques to epidemic models by deriving the exact convergence result of the nonlinear SIS model. We also observe that Theorem 2.1 is a special case for when the infection and recovery rates are linear.

#### A. Monotone Dynamical Systems - A Primer

A well known result from real analysis is that monotone sequences in compact (closed and bounded) subsets of  $\mathbb{R}^n$  converge in  $\mathbb{R}^n$  [58]. This simple, yet powerful result has been fully integrated with the theory of dynamical systems in a series of works [51], [59], [60], [61], [62], [63], [64], [65], [66], [67], which cumulatively form the theory of *monotone dynamical systems* (MDS). The foundations of MDS were laid down in [51], [59], [60], [61], and [62] which study ordinary differential equations, specifically *cooperative* ODE systems. We here provide a brief, informal introduction to such ODE systems, with more details in Appendix B.

A central tool in the theory of MDS is the notion of *generalized cone-orderings*, which extends the concept of monotonicity in vector spaces.

Definition 4.1: Given a convex cone  $K \subset X$  for any vector space X, the cone-ordering  $\leq_K (<_K, \ll_K)$  generated by K is an order relation that satisfies

- (i)  $\mathbf{x} \leq_K \mathbf{y} \iff (\mathbf{y} \mathbf{x}) \in K$ ;
- (ii)  $\mathbf{x} <_K \mathbf{y} \iff \mathbf{x} \leq_K \mathbf{y}$  and  $\mathbf{x} \neq \mathbf{y}$ ; and
- (iii)  $\mathbf{x} \ll_K \mathbf{y} \iff (\mathbf{y} \mathbf{x}) \in \operatorname{int}(K)$ , for any  $\mathbf{x}, \mathbf{y} \in X$ . Note that, ' $\ll_K$ ' implies ' $<_K$ ' and is a stronger relation. Cone-orderings generated by the positive orthant  $K = \mathbb{R}^n_+$  are simply denoted by  $\leq (<, \ll)$ , that is, without the 'K' notation.

Let  $\phi_t(\mathbf{x})$  denote the solution of a dynamical system at some time t > 0 starting from an initial point  $\phi_0(\mathbf{x}) = \mathbf{x} \in \mathbb{R}^n$ .

Definition 4.2: Given a cone-ordering  $\leq_K (<_K, \ll_K)$ , the dynamical system is said to be *monotone* if for every  $\mathbf{x}, \mathbf{y} \in \mathbb{R}^n$  such that  $\mathbf{x} \leq_K \mathbf{y}$ , we have  $\phi_t(\mathbf{x}) \leq_K \phi_t(\mathbf{y})$  for all t > 0. The system is called *strongly monotone* if for all  $\mathbf{x}, \mathbf{y} \in \mathbb{R}^n$  such that  $\mathbf{x} <_K \mathbf{y}$ , we have  $\phi_t(\mathbf{x}) \ll_K \phi_t(\mathbf{y})$  for all t > 0.

The main result from MDS theory says that (almost) every solution trajectory of a *strongly monotone* system always converges to some equilibrium point of the system [44], [59], [65], [66]. If the system has only one stable fixed point, then this in itself is enough to prove global convergence. Monotonicity properties of a dynamical system can therefore be leveraged as an alternative to constructing Lyapunov functions, which is often intractable.

Consider the following autonomous ODE system

$$\dot{\mathbf{x}} = \bar{F}(\mathbf{x}),\tag{9}$$

where  $\bar{F}(\mathbf{x}) = [\bar{f}_i(\mathbf{x})] \in \mathbb{R}^n$  is the vector field. If  $\phi_t(\mathbf{x})$  is the solution of this ODE system, we say the system is *co-operative* 

if it is monotone. There are ways to find out whether an ODE system is co-operative or not. In particular, one can answer this by observing the Jacobian of the vector field [68]. The so-called *Kamke condition* [67] says that (9) is co-operative with respect to the cone-ordering generated by the positive orthant  $K = \mathbb{R}^n_+$  if and only if

$$\frac{\partial \bar{f}_i}{\partial x_i} \ge 0$$
, for all  $i \ne j$ . (10)

While it is not straightforward to obtain such a clean condition for any general convex cone K, one can still deduce the co-operative property of the ODE with respect to any one of the other orthants of  $\mathbb{R}^n$  by observing the signed entries of the Jacobian. We will show how this is done for the bi-virus system (4) later in Section V-A.

If the Jacobian of an ODE system is an irreducible matrix in a subset D of the state space, we say that the ODE system is *irreducible in* D (Definition B.2 in Appendix B). If the ODE system is co-operative in D as well as irreducible in D, then it is strongly monotone in D (Theorem B.4 in Appendix B). To prove convergence properties, we should ideally be able to show that our system is strongly monotone in the entirety of the state space it is contained in, for which we can directly apply the main MDS convergence result. However, this is often not the case, and one needs additional results from MDS literature to prove convergence. These details are deferred to Appendix B.

#### B. Monotonicity and Convergence of SIS Epidemic Models

The following proposition establishes the monotonicity of the single-virus SIS model with non-linear infection and recovery rates with respect to the regular ordering relationship (cone-ordering generated by  $\mathbb{R}^N_+$ ).

Proposition 4.3: The ODE system (6) is cooperative in  $[0,1]^N$  and irreducible in  $(0,1)^N$  with respect to the cone-ordering generated by the positive orthant  $\mathbb{R}^N_+$ .

We now state the convergence criterion for the non-linear single-virus SIS model.

Theorem 4.4: Let  $J_F(\mathbf{x})$  and  $J_Q(\mathbf{x})$  denote the Jacobian matrices of the vector valued infection and recovery rate functions  $F(\mathbf{x})$  and  $Q(\mathbf{x})$  from (6), respectively. Then,

- (i) either  $\lambda(\mathbf{J}_F(\mathbf{0}) \mathbf{J}_Q(\mathbf{0})) \le 0$ , and  $\mathbf{x}^* = 0$  is the globally asymptotically stable fixed point of (6);
- (ii) or  $\lambda(\mathbf{J}_F(\mathbf{0}) \mathbf{J}_Q(\mathbf{0})) > 0$ , and there exists a unique, strictly positive fixed point  $\mathbf{x}^* \gg 0$  such that  $\mathbf{x}^*$  is globally asymptotically stable in  $[0,1]^N \setminus \{\mathbf{0}\}$ .

The proof for Theorem 4.4 utilizes a result from the monotone dynamical systems literature, provided as Theorem C.1 in Appendix C. It was originally proved and applied to linear SIS epidemics in [69] as an alternate proof of the convergence properties of the model for Gonorrhea spread in [2], which is a special case of our non-linear model (6). We can also see this in the following remark.

Remark 4.5: For the single-virus SIS model with linear infection and recovery rates (2), the conditions derived in Theorem 4.4 reduce to those in Theorem 2.1.

*Proof*: By substituting  $F(\mathbf{x}) = \beta \mathbf{A} \mathbf{x}$  and  $Q(\mathbf{x}) = \delta \mathbf{x}$  in (21) (Jacobian of the single-virus system (6), mentioned in

the proof of Theorem 4.4) and evaluating at  $\mathbf{x} = \mathbf{0}$ , we get  $\mathbf{J}_{\bar{F}}(\mathbf{0}) = \mathbf{J}_F(\mathbf{0}) - \mathbf{J}_Q(\mathbf{0}) = \beta \mathbf{A} - \delta \mathbf{I}$ . The condition  $\lambda(\mathbf{J}_F(\mathbf{0}) - \mathbf{J}_Q(\mathbf{0})) = \lambda(\beta \mathbf{A} - \delta \mathbf{I}) > 0 \ (\leq 0)$  can be rewritten as  $\tau > 1/\lambda(\mathbf{A}) \ (\leq 1/\lambda(\mathbf{A}))$  where  $\tau = \beta/\delta$ , which as the same as in Theorem 2.1.

While Theorem 4.4 could be proved using the steps in [2], which were recreated again in [20], it requires first the application of two different Lyapunov functions and also requires proving the uniqueness of the positive fixed point. Alternatively, one could apply Theorem 1 in [70] to establish the uniqueness of the positive fixed point by first showing that the Jacobian of  $\bar{F}(\mathbf{x})$  evaluated at any point  $\mathbf{x}\gg \mathbf{0}$  satisfying  $\bar{F}(\mathbf{x})=\mathbf{0}$ , is Hurwitz. This, combined with Proposition 4.3, could then provide the necessary convergence criterion. However, we maintain that using Theorem C.1 would be a simpler way to derive the same results, whose proof is deferred to Appendix C.

# V. MAIN RESULTS FOR THE NON-LINEAR Bi-VIRUS MODEL

We provide the necessary and sufficient results on the non-linear infection and recovery rates of the bi-virus system (8) for convergence to each of the three different kinds of equilibria: the virus-free, the single-virus equilibrium, and the co-existence equilibrium. However, before stating the main convergence results (proofs deferred to Appendix F in [55]), we establish the monotonicity of the non-linear bi-virus model.

#### A. Monotonicity of the Bi-Virus Epidemic Models

We first revisit the Kamke condition from Section IV-A, in this instance given for a the *southeast cone-ordering* as stated below.

Southeast cone-ordering and the Kamke condition Consider the cone-ordering generated by the convex cone  $K = \{\mathbb{R}^N_+ \times \mathbb{R}^N_-\} \subset \mathbb{R}^{2N}$ . This cone is one of the orthants of  $\mathbb{R}^{2N}$ , and for N = 1, it would correspond to the southeast orthant of  $\mathbb{R}^2$   $(K = \{\mathbb{R}_+ \times \mathbb{R}_-\} \subset \mathbb{R}^2)$ . For any two points  $(\mathbf{x}, \mathbf{y})$ ,  $(\bar{\mathbf{x}}, \bar{\mathbf{y}}) \in \mathbb{R}^{2N}$ , it satisfies the following:

- (i)  $(\mathbf{x}, \mathbf{y}) \leq_K (\bar{\mathbf{x}}, \bar{\mathbf{y}}) \iff x_i \leq \bar{x}_i \text{ and } y_i \geq \bar{y}_i \text{ for all } i \in \mathcal{N};$
- (ii)  $(\mathbf{x}, \mathbf{y}) <_K (\bar{\mathbf{x}}, \bar{\mathbf{y}}) \iff (\mathbf{x}, \mathbf{y}) \leq_K (\bar{\mathbf{x}}, \bar{\mathbf{y}}) \text{ and } (\mathbf{x}, \mathbf{y}) \neq (\bar{\mathbf{x}}, \bar{\mathbf{y}});$
- (iii)  $(\mathbf{x}, \mathbf{y}) \ll_K (\bar{\mathbf{x}}, \bar{\mathbf{y}}) \iff x_i < \bar{x}_i \text{ and } y_i > \bar{y}_i \text{ for all } i \in \mathcal{N}$

This type of cone-ordering is often referred to as the *southeast* cone-ordering, and the corresponding cone K is the *southeast* orthant of  $\mathbb{R}^{2N}$ . As shown in [68], the Kamke condition for determining whether an ODE system is cooperative or not with respect to the positive orthant  $\mathbb{R}^{2N}_+$  can be generalised for cone-orderings generated by any orthant of  $\mathbb{R}^{2N}$ , including the southeast orthant. Once again, this is done by observing the Jacobian of the respective ODE system. Consider the 2N dimensional system given by

$$\dot{\mathbf{x}} = \bar{G}(\mathbf{x}, \mathbf{y})$$
 and  $\dot{\mathbf{y}} = \bar{H}(\mathbf{x}, \mathbf{y})$ ,

where  $\bar{G}(\mathbf{x}, \mathbf{y}) = [\bar{g}_i(\mathbf{x}, \mathbf{y})]$  and  $\bar{H}(\mathbf{x}, \mathbf{y}) = [\bar{h}_i(\mathbf{x}, \mathbf{y})]$  are vector-valued functions in  $\mathbb{R}^N$ . The Kamke condition for this

system with respect to the southeast cone-ordering [68] is

$$\frac{\partial \bar{g}_i}{\partial x_j} \geq 0, \ \frac{\partial \bar{h}_i}{\partial y_j} \geq 0, \ \forall i \neq j, \ \text{and} \ \ \frac{\partial \bar{g}_i}{\partial y_j} \leq 0, \ \frac{\partial \bar{h}_i}{\partial x_j} \leq 0, \ \forall i,j.$$

Roughly speaking, the Jacobian  $J_{GH}(\mathbf{x}, \mathbf{y})$  of the system, evaluated at all points in the state space, should be in the following block matrix form (where the signs are not strict):

$$\mathbf{J}_{\bar{G}\bar{H}} = \begin{bmatrix} * & + & + & - & - & - \\ + & * & + & - & - & - \\ + & * & * & - & - & - \\ - & - & - & * & + & + \\ - & - & - & + & * & * \end{bmatrix}$$
(11)

Note that the state space of the ODE system (4) is given by  $D \triangleq \{(\mathbf{x}, \mathbf{y}) \in [0, 1]^{2N} \mid \mathbf{x} + \mathbf{y} \leq \mathbf{1}\}.$ 

Proposition 5.1: The ODE system (8) (the non-linear bivirus model) is cooperative in D with respect to the southeast cone-ordering. It is also irreducible in Int(D).

*Proof:* For all  $(\mathbf{x}, \mathbf{y}) \in D$  and  $i \neq j \in \mathcal{N}$ , we have

$$\frac{\partial \bar{g}_i(\mathbf{x}, \mathbf{y})}{\partial x_j} = (1 - x_i - y_i) \frac{\partial g_i(\mathbf{x})}{\partial x_j} - \frac{\partial r_i(\mathbf{x})}{\partial x_j} \ge 0,$$
$$\frac{\partial \bar{h}_i(\mathbf{x}, \mathbf{y})}{\partial y_j} = (1 - x_i - y_i) \frac{\partial h_i(\mathbf{y})}{\partial y_j} - \frac{\partial s_i(\mathbf{x})}{\partial y_j} \ge 0$$

since  $\frac{\partial g_i(\mathbf{x})}{\partial x_j} \geq 0$ ,  $\frac{\partial r_i(\mathbf{x})}{\partial x_j} \leq 0$  and  $\frac{\partial h_i(\mathbf{y})}{\partial y_j} \geq 0$ ,  $\frac{\partial s_i(\mathbf{y})}{\partial y_j} \leq 0$  from assumptions (A2) and (A3), and  $(1-x_i-y_i) \geq 0$ . Moreover for all  $i \in \mathcal{N}$ ,

$$\frac{\partial \bar{g}_i}{\partial y_i} = -g_i(\mathbf{x}) \leq 0 \quad \text{and} \quad \frac{\partial \bar{h}_i}{\partial x_i} = -h_i(\mathbf{y}) \leq 0,$$

with  $\partial \bar{g}_i/\partial y_j=\partial \bar{h}_i/\partial x_j=0$ . Thus, the Kamke conditions are satisfied and the system is cooperative in D.

The Jacobian  $\mathbf{J}_{\bar{G}\bar{H}}(\mathbf{x},\mathbf{y})$  of system (4) is written as (12), as shown at the bottom of the next page, where  $\mathbf{S}_{\mathbf{x},\mathbf{y}} \triangleq \mathrm{diag}(\mathbf{1} - \mathbf{x} - \mathbf{y})$ ,  $\mathbf{D}_{G(\mathbf{x})} \triangleq \mathrm{diag}(G(\mathbf{x}))$  and  $\mathbf{D}_{H(\mathbf{y})} \triangleq \mathrm{diag}(H(\mathbf{y}))$ . Since the infection rate functions satisfy assumption (A2) for their corresponding underlying graphs,  $\mathbf{J}_G(\mathbf{x})$  and  $\mathbf{J}_H(\mathbf{y})$  follow the sign structure of  $\mathbf{A}$  and  $\mathbf{B}$  respectively and are irreducible. The off-diagonal blocks of  $\mathbf{J}_{\bar{G}\bar{H}}(\mathbf{x},\mathbf{y})$  are diagonal matrices with non-zero diagonal entries for  $(\mathbf{x},\mathbf{y}) \in \mathrm{Int}(D)$ , and there does not exist a permutation matrix that would transform this into a block upper triangular matrix. Hence, by Definition B.2, the system is irreducible in  $\mathrm{Int}(D)$ , and this completes the proof.

From Proposition 5.1, we deduce that the non-linear bi-virus system of ODEs (8) is co-operative in D, and thus strongly monotone in  $\operatorname{Int}(D)$  in view of Theorem B.4 in Appendix B. This property also extends to the linear bi-virus system (4) which is a special case of (8).

# B. Convergence and Coexistence Properties of the Bi-Virus Model

We are now ready to establish results on convergence properties of the bi-virus model and provide conditions for coexistence of two viruses in the non-linear bi-virus model as in (8). Let  $x^*$  and  $y^*$  be the globally attractive fixed points of the single-virus SIS models that system (8) would reduce to when Virus 2 and 1, respectively, are not present over the network. These systems are given by

$$\dot{\mathbf{x}} = F^x(\mathbf{x}) \triangleq \bar{G}(\mathbf{x}, \mathbf{0}) = \operatorname{diag}(\mathbf{1} - \mathbf{x})G(\mathbf{x}) - R(\mathbf{x}),$$
 (13)

$$\dot{\mathbf{y}} = F^y(\mathbf{y}) \triangleq \bar{H}(\mathbf{0}, \mathbf{y}) = \operatorname{diag}(\mathbf{1} - \mathbf{y})H(\mathbf{y}) - S(\mathbf{y});$$
 (14)

and by Theorem 4.4,  $\mathbf{x}^* = \mathbf{0}$  ( $\mathbf{y}^* = \mathbf{0}$ ) if  $\lambda (\mathbf{J}_G(\mathbf{0}) - \mathbf{J}_R(\mathbf{0})) \leq 0$  (if  $\lambda (\mathbf{J}_H(\mathbf{0}) - \mathbf{J}_S(\mathbf{0})) \leq 0$ ), and  $\mathbf{x}^* \gg \mathbf{0}$  ( $\mathbf{y}^* \gg \mathbf{0}$ ) otherwise.

We first state the result when the virus-free equilibrium is globally attractive. We prove this by presenting simple arguments which require only Theorem 4.4 for SIS model along with the monotonicity properties derived in the previous section, eliminating the need of a Lyapunov based approach.

Theorem 5.2 (Convergence to virus-free equilibria). If  $\lambda(\mathbf{J}_G(\mathbf{0}) - \mathbf{J}_R(\mathbf{0})) \leq 0$  and  $\lambda(\mathbf{J}_H(\mathbf{0}) - \mathbf{J}_S(\mathbf{0})) \leq 0$ , trajectories of (8) starting from any point in D converge to  $(\mathbf{0},\mathbf{0})$ .

We next characterize the conditions when the system globally converges to equilibria when only one of the viruses survives over the network. Let  $\mathbf{S}_{\mathbf{x}} \triangleq \operatorname{diag}(\mathbf{1} - \mathbf{x})$  and  $\mathbf{S}_{\mathbf{y}} \triangleq \operatorname{diag}(\mathbf{1} - \mathbf{y})$  for any  $\mathbf{x}, \mathbf{y} \in \mathbb{R}^N$ . Also denote by  $B_x \triangleq \{(\mathbf{x}, \mathbf{y}) \in D \mid \mathbf{x} > \mathbf{0}\}$  the set of all points  $(\mathbf{x}, \mathbf{y}) \in D$  for which  $x_i > 0$  for some  $i \in \mathbb{N}$ , and let  $B_y \triangleq \{(\mathbf{x}, \mathbf{y}) \in D \mid \mathbf{y} > \mathbf{0}\}$  be a similar set for the  $y_i$  entries.

Theorem 5.3 (Convergence to single-virus equilibria): When  $\lambda(\mathbf{S_{y^*}J}_G(\mathbf{0}) - \mathbf{J}_R(\mathbf{0})) > 0$  and  $\lambda(\mathbf{S_{x^*}J}_H(\mathbf{0}) - \mathbf{J}_S(\mathbf{0})) \leq 0$ ,  $(\mathbf{x^*}, \mathbf{0})$  is globally attractive in  $B_x$ ; that is, every trajectory of system (8) starting from points in  $B_x$  converges to  $(\mathbf{x^*}, \mathbf{0})$ .

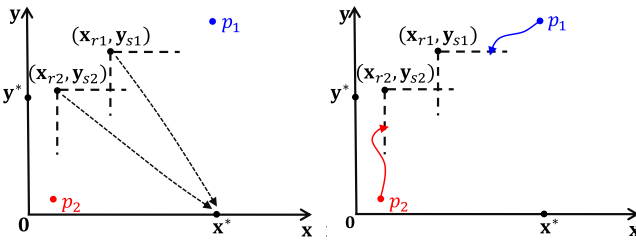
Similarly, when  $\lambda(\mathbf{S_{y^*}J}_G(\mathbf{0}) - \mathbf{J}_R(\mathbf{0})) \leq 0$  and  $\lambda(\mathbf{S_{x^*}J}_H(\mathbf{0}) - \mathbf{J}_S(\mathbf{0})) > 0$  is globally attractive in  $B_y$ .  $\square$ 

Proof: [Sketch of the proof (convergence to  $(\mathbf{x}^*, \mathbf{0})$ )] The idea behind the proof is illustrated in Figure 2. For every  $(\mathbf{x}, \mathbf{y}) \in B_x$  (for example  $p_1$  and  $p_2$  in Figure 2), we construct a point  $(\mathbf{x}_r, \mathbf{y}_s)$  which eventually bounds the trajectory starting from  $(\mathbf{x}, \mathbf{y})$ ; that is, we have  $(\mathbf{x}_r, \mathbf{y}_s) \ll_K \phi_{t_1}(\mathbf{x}, \mathbf{y}) \leq_K (\mathbf{x}^*, \mathbf{0})^8$  for some  $t_1 \geq 0$ . From the monotonicity shown in Proposition 5.1, we have  $\phi_t(\mathbf{x}_r, \mathbf{y}_s) \ll_K \phi_{t+t_1}(\mathbf{x}, \mathbf{y}) \leq_K (\mathbf{x}^*, \mathbf{0})$  for all time  $t \geq 0$ . We prove that the trajectory starting from  $(\mathbf{x}_r, \mathbf{y}_s)$  converges to  $(\mathbf{x}^*, \mathbf{0})$  monotonically, with respect to the southeast cone-ordering (Figure 2(a)). Using this, we show the convergence of trajectories starting from  $(\mathbf{x}, \mathbf{y})$  via a sandwich argument (Figure 2(b)). See Appendix F in [55] for detailed proof.

Finally, we give the necessary and sufficient conditions that guarantee the co-existence of the two viruses in the long run. Let E denote the set of all fixed points of the system in (8).

Theorem 5.4 (Convergence to coexistence equilibria): If  $\lambda \left( \mathbf{S}_{\mathbf{y}^*} \mathbf{J}_G(\mathbf{0}) - \mathbf{J}_R(\mathbf{0}) \right) > 0$  and  $\lambda \left( \mathbf{S}_{\mathbf{x}^*} \mathbf{J}_H(\mathbf{0}) - \mathbf{J}_S(\mathbf{0}) \right) > 0$ , there exist fixed points of system (8)  $(\hat{\mathbf{x}}, \hat{\mathbf{y}}) \gg (\mathbf{0}, \mathbf{0})$  and

<sup>&</sup>lt;sup>7</sup>We consider  $B_x$  as the global domain of attraction instead of D because  $\mathbf{x} = 0$  for all points in the set  $D \setminus B_x$ . Starting from such points the system is no longer a bi-virus epidemic, but a single-virus SIS system for Virus 2.  ${}^8\phi_t(\mathbf{x},\mathbf{y})$  denotes the solution of (4) at  $t \geq 0$ , with initial point ( $\mathbf{x},\mathbf{y}$ ).



tonically  $(\leq_K)$  to  $(\mathbf{x}^*, 0)$ .

(a) For every point  $p_k$ , there is (b) Trajectories starting from  $p_k$ a point  $(\mathbf{x}_{rk}, \mathbf{y}_{sk})$  starting from eventually bounded by  $(\mathbf{x}_{rk}, \mathbf{y}_{sk})$ ; which, trajectories converge mono- monotonicity of the system gives convergence to  $(\mathbf{x}^*, 0)$ .

Fig. 2. Illustration of the convergence to  $(\mathbf{x}^*, 0)$ .

$$(ar{\mathbf{x}},ar{\mathbf{y}})\gg(\mathbf{0},\mathbf{0})$$
 such that 
$$(\mathbf{0},\mathbf{y}^*)\ll_K(\hat{\mathbf{x}},\hat{\mathbf{y}})\leq_K(ar{\mathbf{x}},ar{\mathbf{y}})\ll_K(\mathbf{x}^*,\mathbf{0}),$$

with the possibility that  $(\hat{\mathbf{x}}, \hat{\mathbf{y}}) = (\bar{\mathbf{x}}, \bar{\mathbf{y}})$ . All trajectories of system (8) starting from  $B_x \cap B_y$  converge to the set of coexistence fixed points S $\{(\mathbf{x}_e, \mathbf{y}_e) \in E \mid (\hat{\mathbf{x}}, \hat{\mathbf{y}}) \leq_K (\mathbf{x}_e, \mathbf{y}_e) \leq_K (\bar{\mathbf{x}}, \bar{\mathbf{y}})\}.$ 

The proof of Theorem 5.4 follows similar arguments to that of the previous theorem, and is the first convergence result for coexistence fixed points in the competing SIS literature. Note that while we have convergence to 'a' coexistence equilibrium, it may or may not be unique in the state space. The global convergence is therefore to the set of possible coexistence equilibria, and not necessarily a singular point. Thus, via Theorems 5.2, 5.3 and 5.4 we cover all possible convergence scenarios of the bi-virus SIS system (8), and successfully establish the complete theoretical characterization for the trichotomy of possible outcomes.

# VI. LINEAR INFECTION AND RECOVERY RATES -DISCUSSION AND COMPARISON TO LITERATURE

We now take a look at the special case of the bi-virus epidemic model where infection and recovery rates scale linearly with the local infection probability. This is the most commonly analysed setting in literature [21], [31], [32], [33], [34], [54], and allows us to provide a comprehensive discussion on the related works. With the exception of [54], a line of work seemingly developed concurrently to ours, we observe that most existing works only provide limited results regarding convergence to coexistence equilibria. In what follows, we provide corollaries of Theorems 5.2, 5.3 and 5.4 which characterize convergence to the trichotomy of possible outcomes for the special case of linear infection and recovery rates. These results, along with Figure 3, are reproduced here as they originally were in our previous work [1] which focused only on characterizing the convergence properties in the case of linear infection and recovery rates.

The model considered in this section is the bi-virus system (4) with homogeneous infection and recovery rates.9 While at first this may seem too simplistic compared to the case of linear, heterogeneous rates, 10 and even generic, nonlinear rates analyzed in literature [19], [20], [21], [31], [32], [33], [34], [54], the discussions in the 'Comparison to existing ilterature' subsection will still hold for these more general cases. We only stick to the bi-virus system with homogeneous rates as in (4) to be able to illustrate our results in the form of Figure 3; the axes capturing the parameters of the system. This enables us to better explain our contribution, using visual aids in the form of Figure 3, helping us compare our work with some of the existing literature more effectively, as opposed to presenting any other special case of the bi-virus model.

Consider the linear bi-virus system (4). By setting  $G(\mathbf{x}) =$  $\beta_1 \mathbf{A} \mathbf{x}$ ,  $R(\mathbf{x}) = \delta_1 \mathbf{x}$  and  $H(\mathbf{y}) = \beta_2 \mathbf{B} \mathbf{y}$ ,  $S(\mathbf{y}) = \delta_2 \mathbf{y}$ , we get

$$\mathbf{J}_G(\mathbf{0}) = \beta_1 \mathbf{A}, \quad \mathbf{J}_R(\mathbf{0}) = \delta_1 \mathbf{I},$$

and

$$\mathbf{J}_H(\mathbf{0}) = \beta_2 \mathbf{B}, \ \mathbf{J}_S(\mathbf{0}) = \delta_2 \mathbf{I}.$$

Defining  $\tau_1 \triangleq \beta_1/\delta_1$ ,  $\tau_2 = \Delta\beta_2/\delta_2$ , and plugging in the above expressions for the Jacobians in Theorems 5.2 and 5.3, we have the following Corollaries.

Corollary 6.1: If  $\tau_1 \lambda(\mathbf{A}) \leq 1$  and  $\tau_2 \lambda(\mathbf{B}) \leq 1$ , trajectories of (4) starting from any point in D converge to (0,0). Corollary 6.2: When  $\tau_1 \lambda(\mathbf{S}_{\mathbf{y}^*} \mathbf{A}) > 1$  and  $\tau_2 \lambda(\mathbf{S}_{\mathbf{x}^*} \mathbf{B}) \leq 1$ ,  $(\mathbf{x}^*, \mathbf{0})$  is globally attractive in  $B_x$ ; 11 that is, every trajectory of system (4) starting from points in  $B_x$  converges to  $(\mathbf{x}^*, \mathbf{0})$ .

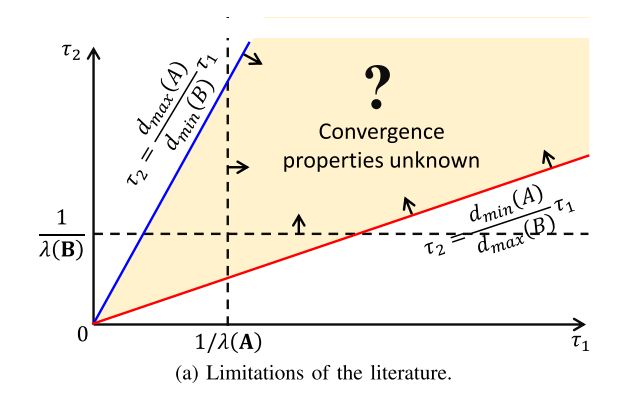
Similarly, when  $\tau_1 \lambda(\mathbf{S}_{\mathbf{v}^*} \mathbf{A}) \leq 1$  and  $\tau_2 \lambda(\mathbf{S}_{\mathbf{x}^*} \mathbf{B}) > 1$ ,  $(\mathbf{0}, \mathbf{y}^*)$  is globally attractive in  $B_y$ . From Corollary 6.2, we can deduce that the threshold values for  $\tau_1$  and  $\tau_2$  below which each of the viruses will die out are given by the equations  $\tau_1 = 1/\lambda(\mathbf{S}_{\mathbf{v}^*}\mathbf{A})$  and  $\tau_2 =$  $1/\lambda(\mathbf{S_{x^*}B})$ , respectively. Figure 3(b) plots these threshold values for Virus 1 (in blue) and Virus 2 (in red) for varying values of  $\tau_1$  and  $\tau_2$ , and partitions the entire parameter space into regions R1 - R6 as shown. When  $\tau_1 > 1/\lambda(\mathbf{A})$  and  $\tau_2 > 1/\lambda(\mathbf{B})$ , for which values of  $\tau_1, \tau_2$  do not lie in regions R1, R2 or R3, the blue curve lies above the red curve as in Figure 3(b). This was originally shown in [18] by deducing that the ratio of slopes of the red and blue curves at point  $(\tau_1, \tau_2) = (1/\lambda(\mathbf{A}), 1/\lambda(\mathbf{B}))$  is less than one. This means

<sup>9</sup>Every infected node  $i \in \mathcal{N}$  infects its susceptible neighbor with the same rate  $\beta_1 > 0$  or  $\beta_2 > 0$ , and in turn recovers with the same rate  $\delta_1 > 0$  or  $\delta_2 > 0$ , depending on whether it is infected by Virus 1 or 2 respectively.

 $^{10}$ The adjacency matrices  ${\bf A}$  and  ${\bf B}$  in (4) can be symmetric, irreducible, weighted; with  $a_{ij}, b_{ij} \geq 0$  (not necessarily 0/1 valued) multiplied by  $\beta_1$  and  $\beta_2$  respectively, being the infection rates from node  $j \to i$  for Viruses 1 and 2. Recovery rates can similarly be heterogenized as  $\delta_1 = [\delta_1^i]$  and  $\delta_2 = [\delta_2^i]$ for Viruses 1 and 2; written as recovery rate matrices diag( $\delta_1$ ) and diag( $\delta_1$ ), respectively.

<sup>11</sup>We consider  $B_x$  as the global domain of attraction instead of D because  $\mathbf{x} = 0$  for all points in the set  $D \setminus B_x$ . Starting from such points the system is no longer a bi-virus epidemic, but a single-virus SIS system for Virus 2.

$$\mathbf{J}_{\bar{G}\bar{H}}(\mathbf{x}, \mathbf{y}) = \begin{bmatrix} \mathbf{S}_{\mathbf{x}\mathbf{y}} \mathbf{J}_{G}(\mathbf{x}) - \mathbf{D}_{G(\mathbf{x})} - \mathbf{J}_{R}(\mathbf{x}) & -\mathbf{D}_{G(\mathbf{x})} \\ -\mathbf{D}_{H(\mathbf{y})} & \mathbf{S}_{\mathbf{x}\mathbf{y}} \mathbf{J}_{H}(\mathbf{y}) - \mathbf{D}_{H(\mathbf{y})} - \mathbf{J}_{S}(\mathbf{y}) \end{bmatrix}, \tag{12}$$



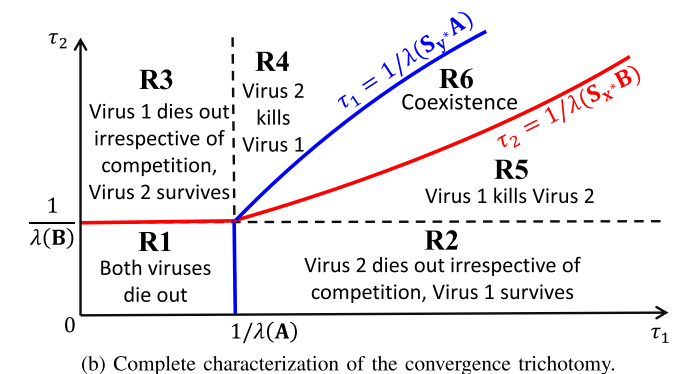


Fig. 3. Characterization of the parameter space.

there exist combinations of  $\tau_1$ ,  $\tau_2$  for which  $\tau_1$  lies to the right of the blue curve  $(\tau_1 \lambda(\mathbf{S_{y^*}A}) > 1)$ , and  $\tau_2$  lies above the red curve  $(\tau_2 \lambda(\mathbf{S_{x^*}B}) > 1)$ . This corresponds to region R6 in Figure 3(b), and our final corollary (derived from Theorem 5.4) shows that for values of  $\tau_1$ ,  $\tau_2$  which lie in R6, we observe convergence to coexistence equilibria.

Corollary 6.3 (Convergence to Coexistence Equilibria): If  $\tau_1 \lambda(\mathbf{S_{y^*}A}) > 1$  and  $\tau_2 \lambda(\mathbf{S_{x^*}B}) > 1$ , there exist fixed points of system (4)  $(\hat{\mathbf{x}}, \hat{\mathbf{y}}) \gg (\mathbf{0}, \mathbf{0})$  and  $(\bar{\mathbf{x}}, \bar{\mathbf{y}}) \gg (\mathbf{0}, \mathbf{0})$  such that

$$(\mathbf{0}, \mathbf{y}^*) \ll_K (\hat{\mathbf{x}}, \hat{\mathbf{y}}) \leq_K (\bar{\mathbf{x}}, \bar{\mathbf{y}}) \ll_K (\mathbf{x}^*, \mathbf{0}),$$

with the possibility that  $(\hat{\mathbf{x}}, \hat{\mathbf{y}}) = (\bar{\mathbf{x}}, \bar{\mathbf{y}})$ . All trajectories of system (4) starting from  $B_x \cap B_y$  converge to the set of coexistence fixed points  $S \triangleq \{(\mathbf{x}_e, \mathbf{y}_e) \in E \mid (\hat{\mathbf{x}}, \hat{\mathbf{y}}) \leq_K (\mathbf{x}_e, \mathbf{y}_e) \leq_K (\bar{\mathbf{x}}, \bar{\mathbf{y}})\}$ .

Comparison to existing literature: Now that we have established all our results, we briefly compare our work with results from [19], [20], which also talk about global convergence to single-virus equilibria. To this end, we first illustrate the limitations of the existing conditions for global convergence in [19] and [20] in Figure 3(a); and use Figure 3(b), where we provide complete characterization of the parameter space, to draw comparisons with our results. We then discuss the works [31], [32], [33], [34] which consider more general models where there can be more than two viruses, but present sharper results in the bi-virus setting. Finally, we will briefly comment on the finiteness of the coexistence equilibria, citing results from [54].

When translated to the setting of linear infection and recovery rates as in 4, the result from [19] says that when  $\tau_1 d_{min}(\mathbf{A}) > \tau_2 d_{max}(\mathbf{B})$ , the Virus 2 is sure to die out (Virus 1 could persist or die out), and similarly when  $\tau_1 d_{max}(\mathbf{A}) < \tau_2 d_{min}(\mathbf{B})$ , the Virus 1 is sure to die out. We illustrate these conditions in Figure 3(a), where Virus 1 (Virus 2) is sure to die out if parameters  $(\tau_1, \tau_2)$  lie above (below) the blue (red) line. Therefore, the entire yellow-shaded region in Figure 3(a), between the blue and red lines, is left uncharacterized in [19].

When A and B are regular graphs with the same degree  $(d_{min} = d_{max} = d)$ , the blue and red lines coincide, making coexistence infeasible. This is also mentioned in [18] where they show that for regular graphs with same degree, the system behaves as if the two graphs were the same rendering coexistence impossible (which is also in line with results in [8]). In contrast, the maximum degree of graphs can also be much larger than the minimum degree (e.g., power law graphs), causing the yellow-shaded space to become very large, possibly spanning almost the entire parameter space.

The main result in [20], when similarly translated to our setting as above, says that when  $\tau_1\lambda(\mathbf{A}) > 1$  and  $\tau_2\lambda(\mathbf{B}) \leq 1$ , Virus 1 survives and Virus 2 dies out. Similarly, when  $\tau_2\lambda(\mathbf{B}) > 1$  and  $\tau_1\lambda(\mathbf{A}) \leq 1$ , Virus 2 survives and Virus 1 dies out. These correspond to regions R2 and R3 in Figure 3(b). However, their results do not cover the convergence properties for  $\tau_1, \tau_2$  which lie in regions R4 – R6. Our Theorems 5.3 and 5.4, through their corresponding corollaries, do account for these values of  $\tau_1, \tau_2$ , and show convergence to  $(\mathbf{0}, \mathbf{y}^*)$ ,  $(\mathbf{x}^*, \mathbf{0})$  or to a coexistence fixed point whenever they lie in regions R4, R5, or R6, respectively.

The works [32], [33] consider the bi-virus epidemic model with heterogeneous linear infection and recovery rates as a special case of their respective multi-virus models. Corollary 2 in [33], a more general version of Theorem 5 in [32] which considers the case where N=2, establishes existence conditions for the coexistence equilibria. These conditions are identical to the ones emerging out of Theorem 5.4 when applied to the bi-virus model considered therein (also identical to the conditions in Corollary 6.3 for the special case of homogeneous, linear infection and recovery rates), and our result can therefore be considered as an extension of those in [32] and [33]; providing convergence results in addition to their existence results. Theorem 6 in [34] (Theorem 8 in [31]) is another interesting result concerning coexistence equilibria, where they show for the special case of viruses spreading over the same (possibly weighted) graph that the survival probability vectors of both the viruses are the same up to a constant multiple; that is, they are parallel.

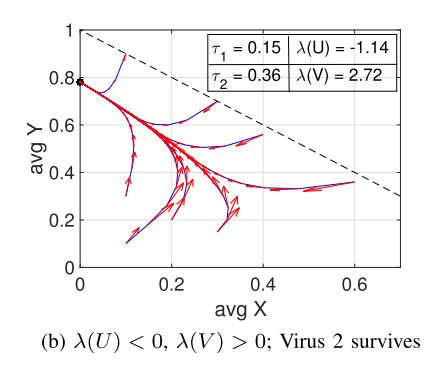
The finiteness of the number of single-virus equilibria is evident from Theorem 4.4, which proves its uniqueness. However, Theorem 5.4 and Corollary 6.3 do not explicitly show that coexistence equilibria are finitely many, let alone

<sup>&</sup>lt;sup>12</sup>Note that  $\tau_1\lambda(\mathbf{S_{y^*}A}) \leq 1$  and  $\tau_2\lambda(\mathbf{S_{x^*}B}) \leq 1$  is only possible in region R1, since it is the only region where  $\tau_1$  can lie to the left of the blue curve, and  $\tau_2$  can lie below the red curve. This effectively reduces the expressions to  $\tau_1\lambda(\mathbf{A}) \leq 1$  and  $\tau_2\lambda(\mathbf{B}) \leq 1$ , the conditions for convergence to the virus-free equilibrium as in Corollary 6.1.

TABLE I
SUMMARY OF INFECTION AND RECOVERY RATE FUNCTIONS CHOSEN

1	`	$\tau_{*} = 1.00$	$\lambda(U) = 3.43$
8.0	V	$\tau_2 = 0.15$	$\lambda(V) = -0.52$
≥ 0.6	1	<i>^</i>	
> 0.6 × 0.4	1		
0.2			
_ ر			
0	0.2	0.4	0.6
	Y nve		

(a)  $\lambda(U) > 0$ ,  $\lambda(V) < 0$ ; Virus 1 survives



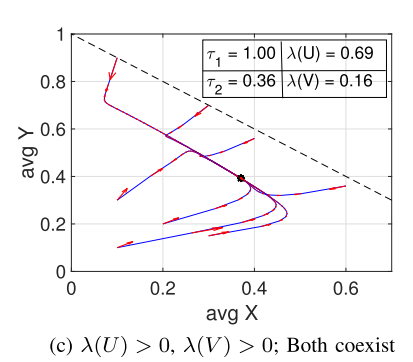


Fig. 4. Phase plots for a system with linear infection and recovery rates (CASE 1) on the AS-733 graph.

uniqueness.<sup>13</sup> For linear, heterogeneous infection and recovery rates, Theorem 3.6 in [54] uses novel techniques from algebraic geometry to prove that the coexistence equilibria are finitely many for all possible values of infection and recovery rates that do not lie in an algebraic set of measure zero. However, this remains an open problem for general, non-linear infection and recovery rate functions satisfying (A1)–(A5).

In summary, without our Theorems 5.3 and 5.4, convergence results from literature fail to characterize a sizeable portion of the parameter space as shown in Figure 3(a) by the '?' region (part of the shaded region surrounded by the arrows). The parameters leading to coexistence are entirely contained in this region as well - explaining the dearth of convergence results for such equilibria in the existing literature.

## VII. NUMERICAL RESULTS

In this section, we present simulation results to support our theoretical findings for the bi-virus SIS model for combinations of non-linear as well as linear infection and recovery rates. To this end, we consider an undirected, connected graph (103 nodes, 239 edges), called Autonomous System (AS-733), from the SNAP repository [71]. For both the linear and non-linear bi-virus model, we generate an additional graph, overlaid on the same set of nodes, by modifying the original graph (AS-733-A with  $\lambda(\mathbf{A}) = 12.16$ ), removing and adding edges while ensuring connectivity between the nodes. The new additional graph, AS-733-B, has 741 edges with  $\lambda(\mathbf{B}) = 15.53$ . Note that since our theoretical results hold for any general graphs, we only use this set as example graphs to numerically demonstrate the convergence properties. Similar numerical results can indeed be obtained for any other networks (such as social networks).

We test the convergence dynamics of the bi-virus model over a range of combinations of linear and non-linear infection and recovery rates. To this end, we consider three different bi-virus models, and Table I summarizes the three cases with the corresponding infection and recovery rate functions as shown. Note that for non-linear infection and recovery rates, we consider the logarithmic and polynomial functions briefly mentioned in Section III, to ensure that our three cases satisfy assumptions (A1)–(A5).

For each of the three cases, we construct combinations of parameters ( $\tau_1$  or  $\tau_2$  for linear rates, and  $\alpha_1$  or  $\alpha_2$  for non-linear rates), to develop three convergence scenarios, that satisfy the assumptions of Theorems 5.3 and 5.4. These three scenarios correspond to global convergence of the bi-virus system to fixed points where (a) Virus 1 is the surviving epidemic (which spreads on graph AS-733-A), (b) Virus 2 is the surviving epidemic (which spreads on graph AS-733-B), (c) both viruses coexist, (where Virus 1 spreads on graph AS-733-A and Virus 2 on AS-733-B). Parameters corresponding to these three scenarios are provided in the table inset in Figures 4–6(a)–(c) corresponding to the three cases.

To visualize our system in two dimensions, we use  $avgX \triangleq (1/N) \sum_{i \in \mathcal{N}} x_i$  on the x-axis, and  $avgY \triangleq (1/N) \sum_{i \in \mathcal{N}} y_i$  on the y-axis. We plot trajectories of the bi-virus system starting from different initial points in the state space D to observe their convergence, with red arrows representing the trajectories' direction of movement at various time intervals. Here, the state space D is the region that lies below the dotted-line (for example, in Figure 4), ensuring  $x_i + y_i \leq 1$  for all  $i \in \mathcal{N}$ , for every initial point. To ensure that the convergences observed in our phase plots match the conditions laid out in Theorems 5.3 and 5.4, we track the eigenvalues  $\lambda(\mathbf{U}) \triangleq \lambda(\mathbf{S_{y^*}J}_G(0) - \mathbf{J}_R(0))$  and  $\lambda(\mathbf{V}) \triangleq \lambda(\mathbf{S_{x^*}J}_H(0) - \mathbf{J}_S(0))$ .  $\lambda(\mathbf{U}) (\lambda(\mathbf{V}))$  being positive or negative corresponds to Virus 1 (Virus 2) surviving or dying out, respectively.

<sup>&</sup>lt;sup>13</sup>In Section VII, we show with the aid of simulation results that the coexistence equilibria are indeed not unique in general.

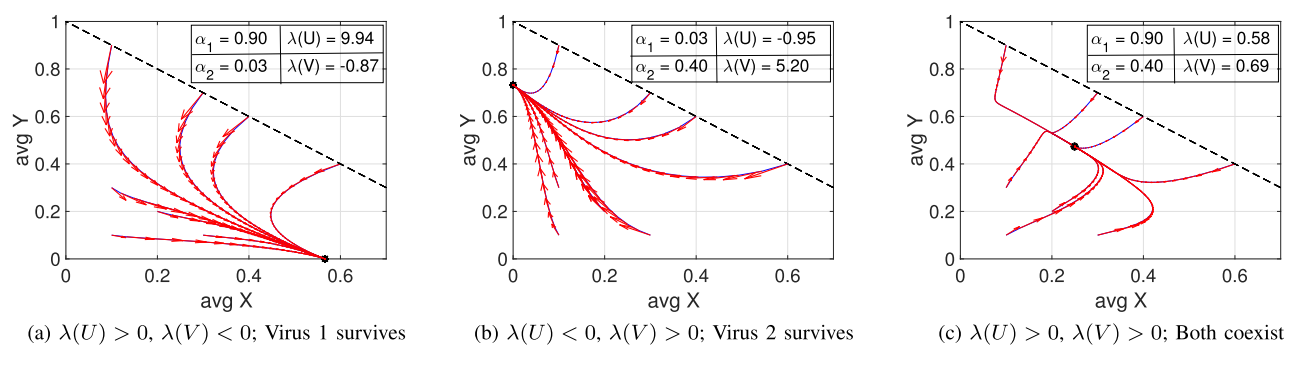


Fig. 5. Phase plots for a system with non-linear infection and linear recovery rates (CASE 2) on the AS-733 graph.

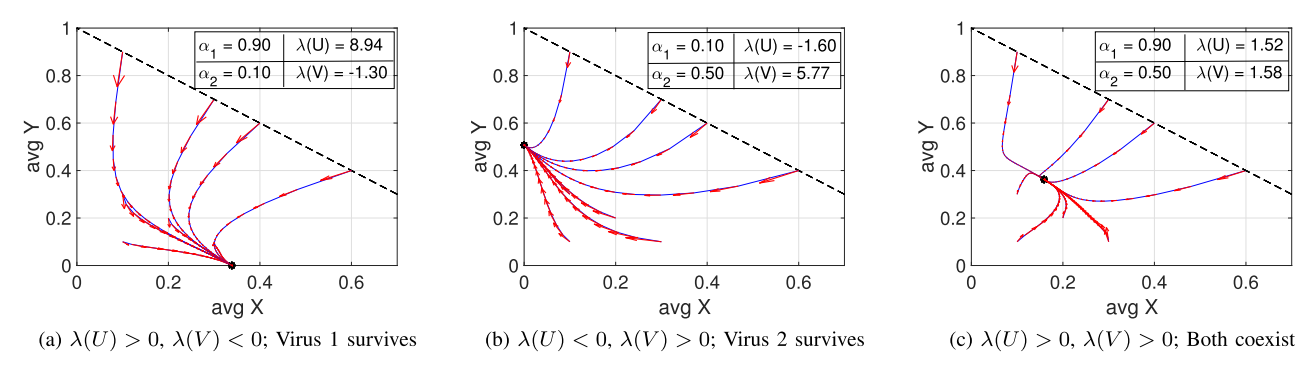


Fig. 6. Phase plots for a system with non-linear infection and recovery rates (CASE 3) on the AS-733 graph.

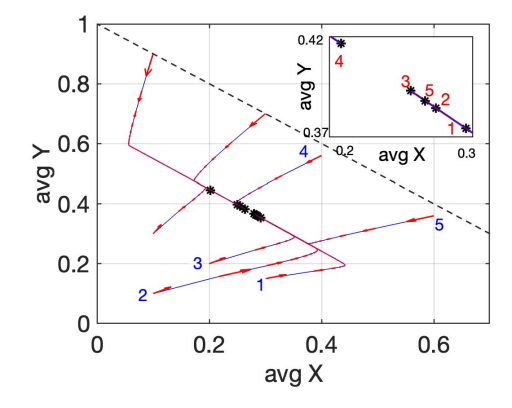


Fig. 7. Coexistence condition with Multiple equilibrium points.

In Figures 4–6(a)–(c), we show numerical results for the three cases, respectively. Figures 4–6(a) and 4–6(b) show convergence to the two different single-virus equilibria, where the parameters therein satisfy the two set of conditions as in Theorem 5.3. Figures 4–6(c) show convergence to the coexistence equilibria, which also satisfies the coexistence conditions as outlined in Theorem 5.4. We observe a unique coexistence equilibrium when the viruses are competing over graphs AS-733-A and AS-733-B, for which the eigenvalues  $\lambda(\mathbf{A})$  and  $\lambda(\mathbf{B})$  are significantly different. Interestingly, we also observe multiple coexistence equilibria as shown in Figure 7. We obtain this result by creating another additional graph by modifying the original graph AS-733-A such that the eigenvalue of this new graph is as close to the original one where this new graph AS-733-C has 259 edges with

 $\lambda(\mathbf{C}) = 12.26$ . The 'upper left' and 'lower right' coexistence fixed points characterize the set S of all such equilibria, as in Theorem 5.4. This can be seen more closely in the inset in Figure 7, where the number beside each fixed point (in red) corresponds to the different initial starting points (in blue) of the trajectories. Thus, convergence to set S occurs globally over the state space, but exactly which coexistence fixed point the system converges to is dependent on the initial point. We are thus able to observe all possible convergence scenarios from Section V-B, including multiple coexistence equilibria.

# VIII. CONCLUDING REMARKS

By utilizing the techniques from Monotone Dynamical Systems (MDS), in this paper, we show that a generic bi-virus epidemic model with non-linear infection and recovery rates is monotone with respect to a specially constructed partial ordering. This monotonicity allows us to give necessary and sufficient conditions on the non-linear infection and recovery rates, and thus completely characterize the entire parameter space of the bi-virus system, a contrast to the usual Lyapunov based approach. We bridge the gap between linear stability properties and global convergence results (or lack thereof) for the bi-virus model with non-linear rates (including the special case with linear rates) in the literature, and succeed in providing a complete characterization of the trichotomy of possible outcomes for such competing epidemics - a well known open problem. Our results demonstrate how powerful these alternative proving techniques can be, compared to classical Lyapunov approaches; and we note that it may be worth exploring such monotonicity properties in other dynamics on graphs as well, where competition is a general theme. Additionally, establishing a rigorous relationship between the SIS ODE models with non-linear rates as studied in this paper, and the correct probabilistic dynamics describing these non-linear rates, is of interest in order to complete the theoretical pictures for SIS models with non-linear rates.

#### APPENDIX A

#### DFR PROCESSES AS NON-LINEAR RECOVERY RATES

In this appendix, we form the connection between *failure* rates from reliability theory [72], and the infection duration at any node in SIS type epidemics. To this end, we start by formally defining the term *failure* rate.

Definition A.1 [72]: Let T > 0 be any continuous random variable with distribution  $F_T(s) = \mathbb{P}(T \leq s)$ , and density function  $f_T(s)$  for all s > 0, with  $\bar{F}_T(s) = 1 - F_T(s) = \mathbb{P}(T > s)$ . Then, the failure rate at any given time s > 0 is defined as

$$r_T(s) \triangleq \frac{f_T(s)}{\bar{F}_T(s)}.$$
 (15)

We say T has a decreasing/increasing failure rate (DFR/IFR) if  $r_T(s)$  is a decreasing/increasing function of s > 0.

When T is the lifetime of a system, the DFR case corresponds to the system aging negatively. This means that as time elapses, the residual time (time till the system fails) is more likely to increase rather than decrease. T could also have an interpretation in the context of node recovery. For the linear SIS epidemic model as in (1), consider an infected node  $i \in \mathcal{N}$  and define  $T \triangleq \text{time}$  taken for node i to recover (random), with  $f_T(s)$  and  $\bar{F}_T(s)$  as in Definition A.1. Loosely speaking, we can ignore the infection rate terms in (1) to take a closer look at the recovery process via the ODE

$$\dot{x}_i(s) = -\delta x_i(s),\tag{16}$$

with the initial condition  $x_i(0)=1$  (implying that node i is last infected at time s=0). The ODE (16) has an exact solution for all s>0, given by  $x_i(s)=e^{-\delta s}$ . This solution allows us to interpret  $x_i$  as the cumulative distribution function (CCDF) of an exponential random variable with rate  $\delta>0$ . Using this interpretation, we have  $x_i(s)=P(T>s)=\bar{F}_T(s)$ , and  $-\dot{x}_i(s)=f_T(s)$ . (16) can then be rewritten as

$$r_T(s) = \frac{-\dot{x}_i(s)}{x_i(s)} = \delta,$$

for any s > 0. T is thus exponentially distributed, and has a constant failure rate (it is both DFR and IFR).

We now consider the case where the random variable T is defined for the more general SIS epidemic model with non-linear recovery rate  $q_i(x_i)$  for node i.<sup>15</sup> Ignoring the infection rate terms in (5) like before, we obtain

$$\dot{x}_i(s) = -q_i\left(x_i(s)\right),\tag{17}$$

retaining the previous interpretation of  $x_i$  as the CCDF of T. This can be further rearranged to obtain an expression for the failure rate as

$$r_T(s) = \frac{-\dot{x}_i(s)}{x_i(s)} = \frac{q_i(x_i(s))}{x_i(s)}$$

for any s > 0. From Definition A.1 we know T is DFR if  $r_T(s)$  is decreasing in s > 0. Supposing  $q_i$  is such that T is indeed DFR,  $\log(r_T(s))$  is also decreases in s, and we get

$$\frac{d}{ds}\log(r_T(s)) = \frac{q_i'(x_i(s))\dot{x}_i(s)}{q(x_i(s))} - \frac{\dot{x}_i(s)}{x_i(s)} \le 0,$$

where  $q_i'(x_i(s))$  denotes the derivative with respect to  $x_i$ . Since  $\dot{x}_i(s) = -q_i(x_i(s))$  from (17) and  $q_i'(x(s)) \geq 0$  from (A3), rearranging the previous equation gives us following the condition for T to be DFR

$$x_i q_i'(x_i) - q_i(x_i) \ge 0.$$
 (18)

In (18), the (s) notation has been suppressed for clarity. Since  $q_i(0) = 0$ , the convexity of  $q_i$  with respect to  $x_i$  implies (18).

Roughly speaking, the DFR case (which also includes linear recovery rates as in (1)) is a subclass of recovery rate functions  $q_i(\mathbf{x})$  satisfying assumptions (A1)–(A5). Even though the above steps may not be exact, they provide intuition on how infections which fester and grow worse with time form part of our modelling assumptions in Section III.

#### APPENDIX B

#### RESULTS FROM MDS AND COOPERATIVE SYSTEMS

*Definition B.1 ([44], [51], [63]):* A flow  $\phi$  is said to be **monotone** if for all  $\mathbf{x}, \mathbf{y} \in \mathbb{R}^n$  such that  $\mathbf{x} \leq_K \mathbf{y}$  and any  $t \geq 0$ , we have  $\phi_t(\mathbf{x}) \leq_K \phi_t(\mathbf{y})$ .

If the flow represents the solution of an ODE system, we say that the ODE system is **co-operative**.

Definition B.2: Consider the system (9) and let  $\mathbf{J}F(\mathbf{x}) \triangleq [df_i(\mathbf{x})/dx_j]$  be the Jacobian of the right hand side evaluated at any point  $\mathbf{x} \in \mathbb{R}^n$ . We say that (9) is an **irreducible ODE** in set  $D \in \mathbb{R}^n$  if for all  $\mathbf{x} \in D$ ,  $\mathbf{J}F(\mathbf{x})$  is an irreducible matrix.

Definition B.3: [44], [63], [67] The flow  $\phi$  is said to be **strongly monotone** if it is monotone, and for all  $\mathbf{x}, \mathbf{y} \in \mathbb{R}^n$  such that  $\mathbf{x} <_K \mathbf{y}$ , and time  $t \ge 0$ , we have  $\phi_t(\mathbf{x}) \ll_k \phi_t(\mathbf{y})$ .

Theorem B.4: [44], [63], [67] Let (9) be irreducible and co-operative in some set  $D \subset \mathbb{R}^n$ . Then the solution  $\phi$  (restricted to  $t \geq 0$ ) is strongly monotone.

As part of the main result of monotone dynamical systems, trajectories of strongly monotone systems, starting from almost anywhere (in the measure theoretic sense) in the state space, converge to the set of equilibrium points [44], [59], [65], [66]. However, often the systems are strongly monotone only in the interior of the state spaces instead of the entirety of the state space. In such cases, the following results are useful.

Proposition B.5: (Proposition 3.2.1 in [67]) Consider the ODE system (9) which is cooperative in a compact set  $D \subset \mathbb{R}^n$  with respect to some cone-ordering, and let  $<_r$  stand for any of the order relations  $\leq_K, <_K, \ll_K$ . Then,  $P_+ \triangleq \{\mathbf{x} \in D \mid \mathbf{0} <_r F(\mathbf{x})\}$  and  $P_- \triangleq \{\mathbf{x} \in D \mid F(\mathbf{x}) <_r \mathbf{0}\}$  are

 $<sup>^{14} \</sup>mbox{When } T \sim \exp(\delta), \mbox{ we have } \bar{F}_T(s) = P(T>s) = e^{-\delta s}.$ 

<sup>&</sup>lt;sup>15</sup>Note that this is the special case where  $q_i$  is only a function of  $x_i$ , not of  $x_i$  for neighbors j of node i.

positively invariant, and the trajectory  $\{\phi_t(\mathbf{x})\}_{t\geq 0}$  for any point  $\mathbf{x} \in P_+$  or  $\mathbf{x} \in P_-$  converges to an equilibrium.

Theorem B.6: (Theorem 4.3.3 in [67]) Let (9) be cooperative (with respect to some cone-ordering  $\leq_K$ ) in a compact set  $D \subset \mathbb{R}^n$  and let  $\mathbf{x}_0 \in D$  be an equilibrium point. Suppose that  $s \triangleq \lambda(\mathbf{J}F(\mathbf{x}_0)) > 0$  (i.e.  $\mathbf{x}_0$  is an unstable fixed point) and there is an eigenvector  $\mathbf{v} \gg_K \mathbf{0}$  such that  $\mathbf{J}F(\mathbf{x}_0)\mathbf{v} = s\mathbf{v}$ . Then, there exists  $\epsilon_0 \in (0, \epsilon]$  and another equilibrium point  $\mathbf{x}_e$  such that for each  $r \in (0, \epsilon_0]$ , the solution  $\phi_t(\mathbf{x}_r)$  has the following properties:

- (1)  $\mathbf{x}_r \ll_K \phi_{t_1}(\mathbf{x}_r) \ll_K \phi_{t_2}(\mathbf{x}_r) \ll_K \mathbf{x}_e$ , for any  $0 < t_1 < t_2$ .
- (2)  $d\phi_t(\mathbf{x}_r)/dt \gg_K \mathbf{0}$ , for any t > 0.
- (3)  $\phi_t(\mathbf{x}_r) \to \mathbf{x}_e$ , as  $t \to \infty$ .

# APPENDIX C PROOFS OF THE RESULTS IN SECTION IV

**Proof of Proposition 4.3:** To prove that system (6) is co-operative with respect to the positive orthant, we show that it satisfies Kamke's condition in (10). Differentiating the right hand side of (5) with respect to  $x_i$ , we get

$$\frac{\partial \bar{f}_i(\mathbf{x})}{\partial x_j} = (1 - x_i) \frac{\partial f_i(x)}{\partial x_j} = \frac{\partial q_i(\mathbf{x})}{\partial x_j}.$$

This corresponds to the (ij)'th off-diagonal entry of the Jacobian  $\mathbf{J}_F(\mathbf{x})$  evaluated at  $\mathbf{x} \in [0,1]^N$ . It is non-negative for any  $i \neq j \in \mathcal{N}$  since  $(1-x_i) \geq 0$  and due to assumption (A3), and the ODE (6) is therefore co-operative in  $[0,1]^N$  with respect to the regular cone ordering.

From assumption (A3),  $\mathbf{J}_{\bar{F}}(\mathbf{x})_{ij}$  is also strictly positive for any  $\mathbf{x} \in (0,1)^N$  whenever  $a_{ij} > 0$ . This means that  $\mathbf{J}_{\bar{F}}(\mathbf{x})$ , and as a consequence the ODE system, is irreducible for any  $\mathbf{x} \in (0,1)^N$ .

To derive the convergence properties of the non-linear SIS model, we make use of a result form [69], rewritten below in a simpler form suitable for our setting.

Theorem C.1 (Theorem 4 in [69]): Consider a generic ODE system (9) invariant to some subset  $S \subset \mathbb{R}^N_+$ , and let  $\mathbf{J}_{\bar{F}}$  stand for its Jacobian matrix. Suppose that:

- (C1)  $f_i(\mathbf{x}) \geq 0$  for all  $\mathbf{x} \geq 0$  with  $x_i = 0$ ;
- (C2) for all  $\mathbf{x} \gg \mathbf{0}$  in S,  $\alpha \in (0,1)$ , it satisfies  $\mathbf{J}_{\bar{F}}(\mathbf{x})_{ij} \leq \mathbf{J}_{\bar{F}}(\alpha \mathbf{x})_{ij}$  for all  $i, j \in \mathcal{N}$ , with strict inequality for at least one pair of i, j;
- (C3) for all  $\mathbf{u} \ll \mathbf{w}$  in S, it satisfies  $\mathbf{J}_{\bar{F}}(\mathbf{w}) \leq \mathbf{J}_{\bar{F}}(\mathbf{u})$ ;
- (C4) it is co-operative in S with respect to the regular ordering relation, and irreducible in Int(S).

Then, exactly one of the following outcomes occurs:

- (i)  $\phi_t(\mathbf{x})$  is unbounded for all  $\mathbf{x} \in S \setminus \{\mathbf{0}\}$ ;
- (ii)  $\phi_t(\mathbf{x}) \to \mathbf{0}$  as  $t \to \infty$ , for all  $\mathbf{x} \in S \setminus \{\mathbf{0}\}$ ;
- (iii) There exists a unique, strictly positive fixed point  $\mathbf{x}^* \gg \mathbf{0}$  such that  $\phi_t(\mathbf{x}) \to \mathbf{x}^*$  as  $t \to \infty$ , for all  $\mathbf{x} \in S \setminus \{\mathbf{0}\}$ .

We now use the above to prove Theorem 4.4.

*Proof of Theorem 4.4:* We prove Theorem 4.4 by showing that it satisfies conditions (C1)-(C4) of Theorem C.1, and then performing stability analysis to evaluate conditions for each of the three possible outcomes therein.

From Proposition (4.3), we know that (6) already satisfies (C4). The right hand side of (5) satisfies (C1) because  $q_i(x_i) = 0$  when  $x_i = 0$ , and because  $(1 - x_i)$  and  $f_i(\mathbf{x})$  are all non-negative for any  $\mathbf{x} \in [0,1]^N$ . To check whether (C2) and (C3) is satisfied, observe that from assumptions (A2)–(A5), we have

$$\mathbf{J}_F(\mathbf{u}) > \mathbf{J}_F(\mathbf{w}) \tag{19}$$

$$\mathbf{J}_Q(\mathbf{u}) < \mathbf{J}_Q(\mathbf{w}) \tag{20}$$

for all  $\mathbf{u} < \mathbf{w}$ .<sup>16</sup> Here,  $\mathbf{J}_Q$  is a diagonal matrix since  $\partial q_i/\partial x_j = 0$  for all  $i \neq j \in \mathcal{N}$ .

Denote by  $\mathbf{J}_{\bar{F}}$  the Jacobian matrix of system (6). Note that for any point  $\mathbf{x} \in [0,1]^N$ , we have

$$\mathbf{J}_{\bar{F}}(\mathbf{x}) = \operatorname{diag}(\mathbf{1} - \mathbf{x})\mathbf{J}_{F}(\mathbf{x}) - \operatorname{diag}(F(\mathbf{x})) - \mathbf{J}_{Q}(\mathbf{x})$$
 (21)

Combining the above with (19) and (20), we have for any points  $\mathbf{u} < \mathbf{w}$  that

$$\begin{split} \mathbf{J}_{\bar{F}}(\mathbf{u}) &= \operatorname{diag}(\mathbf{1} - \mathbf{u})\mathbf{J}_{F}(\mathbf{u}) - \operatorname{diag}\left(F(\mathbf{u})\right) - \mathbf{J}_{Q}(\mathbf{u}) \\ &> \operatorname{diag}(\mathbf{1} - \mathbf{w})\mathbf{J}_{F}(\mathbf{w}) - \operatorname{diag}\left(F(\mathbf{u})\right) - \mathbf{J}_{Q}(\mathbf{w}) \\ &\geq \operatorname{diag}(\mathbf{1} - \mathbf{w})\mathbf{J}_{F}(\mathbf{w}) - \operatorname{diag}\left(F(\mathbf{w})\right) - \mathbf{J}_{Q}(\mathbf{w}) \\ &= \mathbf{J}_{\bar{F}}(\mathbf{w}), \end{split}$$

where the first inequality is due to  $(1-\mathbf{u}) > (1-\mathbf{w})$  and (19) and (20). The second inequality is from the non-negativity and monotonicity assumptions (A2) and (A3) implying  $F(\mathbf{u}) \leq F(\mathbf{w})$ . Since  $\mathbf{J}_{\bar{F}}(\mathbf{u}) > \mathbf{J}_{\bar{F}}(\mathbf{w})$  for any  $\mathbf{u} < \mathbf{w}$ , this is enough to satisfy both conditions (C2) and (C3).

Since system (6) satisfies (C1)–(C4), Theorem C.1 applies. Since the system is invariant in  $[0,1]^N$ , which is a bounded subset of  $\mathbb{R}^N$ , outcome (i) of Theorem C.1 never occurs. From assumption (A1), the vector  $\mathbf{0} = [0, \cdots, 0]^T$  (the virus-free equilibrium) is always a fixed point of the system. We now find conditions under which trajectories of (6) starting from anywhere in  $[0,1]^N\setminus\{\mathbf{0}\}$  converge to either zero, or to a unique strictly positive fixed point (outcomes (ii) and (iii) in Theorem C.1 respectively), by check the stability properties of the system.

The virus-free fixed point zero is unstable [73] when  $\lambda(\mathbf{J}_{\bar{F}}(\mathbf{0})) = \lambda(\mathbf{J}_{F}(\mathbf{0}) - \mathbf{J}_{Q}(\mathbf{0})) \leq 0$ . Under this condition, outcome (ii) in Theorem C.1 is not possible, and there exists a unique, strictly positive fixed point  $\mathbf{x}^* \gg \mathbf{0}$  which is globally asymptotically stable in  $[0,1]^N \setminus \{\mathbf{0}\}$ . Conversely when zero is a stable fixed point, that is when  $\lambda(\mathbf{J}_{\bar{F}}(\mathbf{0})) = \lambda(\mathbf{J}_{F}(\mathbf{0}) - \mathbf{J}_{Q}(\mathbf{0})) > 0$ , it is globally attractive.

## REFERENCES

- [1] V. Doshi, S. Mallick, and D. Y. Eun, "Competing epidemics on graphs—Global convergence and coexistence," in *Proc. IEEE Conf. Comput. Commun. (INFOCOM)*, May 2021, pp. 1–10.
- [2] A. Lajmanovich and J. A. Yorke, "A deterministic model for Gonorrhea in a nonhomogeneous population," *Math. Biosci.*, vol. 28, nos. 3–4, p. 221–236, 1976.
- [3] H. W. Hethcote, "The mathematics of infectious diseases," SIAM Rev., vol. 42, no. 4, pp. 599–653, 2000, doi: 10.1137/S0036144500371907.

<sup>16</sup>Here, the ordering between matrices  $\mathbf{M}^a < \mathbf{M}^b$  means  $\mathbf{M}^a_{ij} \leq \mathbf{M}^b_{ij}$  with the inequality being strict for at least one pair of i,j.

- [4] M. Garetto, W. Gong, and D. Towsley, "Modeling malware spreading dynamics," in *Proc. 32nd Annu. Joint Conf. IEEE Comput. Commun. Societies (INFOCOM)*, San Francisco, CA, USA, May 2003, pp. 1869–1879.
- [5] L.-X. Yang, X. Yang, J. Liu, Q. Zhu, and C. Gan, "Epidemics of computer viruses: A complex-network approach," *Appl. Math. Comput.*, vol. 219, no. 16, pp. 8705–8717, Apr. 2013.
- [6] S. Hosseini and M. A. Azgomi, "A model for malware propagation in scale-free networks based on rumor spreading process," *Comput. Netw.*, vol. 108, pp. 97–107, Oct. 2016.
- [7] K. R. Apt and E. Markakis, "Diffusion in social networks with competing products," in *Proc. Int. Symp. Algorithmic Game Theory*, Oct. 2011, pp. 212–223.
- [8] B. A. Prakash, A. Beutel, R. Rosenfeld, and C. Faloutsos, "Winner takes all: Competing viruses or ideas on fair-play networks," in *Proc. 21st Int. Conf. World Wide Web*, Apr. 2012, pp. 1037–1046.
- [9] S. F. Ruf, K. Paarporn, P. E. Pare, and M. Egerstedt, "Dynamics of opinion-dependent product spread," in *Proc. IEEE 56th Annu. Conf. Decis. Control (CDC)*, Melbourne, VIC, Australia, Dec. 2017, pp. 2935–2940.
- [10] D. Trpevski, W. K. S. Tang, and L. Kocarev, "Model for rumor spreading over networks," *Phys. Rev. E, Stat. Phys. Plasmas Fluids Relat. Interdiscip. Top.*, vol. 81, no. 5, May 2010, Art. no. 056102.
- [11] L. J. Zhao, H. X. Cui, X. Y. Qiu, X. L. Wang, and J. J. Wang, "SIR rumor spreading model in the new media age," *Phys. A*, vol. 392, no. 4, pp. 995–1003, Feb. 2013.
- [12] X. Lin, Q. Jiao, and L. Wang, "Opinion propagation over signed networks: Models and convergence analysis," *IEEE Trans. Autom. Control*, vol. 64, no. 8, pp. 3431–3438, Aug. 2019.
- [13] I. Koprulu, Y. Kim, and N. B. Shroff, "Battle of opinions over evolving social networks," *IEEE/ACM Trans. Netw.*, vol. 27, no. 2, pp. 532–545, Apr. 2019.
- [14] S. Banerjee, A. Chatterjee, and S. Shakkottai, "Epidemic thresholds with external agents," in *Proc. IEEE Conf. Comput. Commun. (INFOCOM)*, Toronto, ON, Canada, Apr. 2014, pp. 2202–2210.
- [15] A. Ganesh, L. Massoulie, and D. Towsley, "The effect of network topology on the spread of epidemics," in *Proc. IEEE 24th Annu. Joint Conf. IEEE Comput. Commun. Societies.*, Miami, FL, USA, Dec. 2005, pp. 1455–1466.
- [16] M. Draief and L. Massoulié, Epidemics and Rumours in Complex Networks, 1st ed. Cambridge, U.K.: Cambridge Univ. Press, 2010.
- [17] F. D. Sahneh, C. Scoglio, and P. V. Mieghem, "Generalized epidemic mean-field model for spreading processes over multilayer complex networks," *IEEE/ACM Trans. Netw.*, vol. 21, no. 5, pp. 1609–1620, Oct. 2013.
- [18] F. D. Sahneh and C. Scoglio, "Competitive epidemic spreading over arbitrary multilayer networks," *Phys. Rev. E, Stat. Phys. Plasmas Fluids Relat. Interdiscip. Top.*, vol. 89, no. 6, 2014, Art. no. 062817.
- [19] A. Santos, J. M. F. Moura, and J. M. F. Xavier, "Bi-virus SIS epidemics over networks: Qualitative analysis," *IEEE Trans. Netw. Sci. Eng.*, vol. 2, no. 1, pp. 17–29, Jan. 2015.
- [20] L.-X. Yang, X. Yang, and Y. Y. Tang, "A bi-virus competing spreading model with generic infection rates," *IEEE Trans. Netw. Sci. Eng.*, vol. 5, no. 1, pp. 2–13, Jan./Mar. 2018.
- [21] J. Liu, P. E. Pare, A. Nedic, C. Y. Tang, C. L. Beck, and T. Basar, "Analysis and control of a continuous-time bi-virus model," *IEEE Trans. Autom. Control*, vol. 64, no. 12, pp. 4891–4906, Dec. 2019.
- [22] P. Van Mieghem, "The N-intertwined SIS epidemic network model," Computing, vol. 93, nos. 2–4, pp. 147–169, Dec. 2011.
- [23] J. Omic and P. Van Mieghem, "Epidemic spreading in networks— Variance of the number of infected nodes," Delft Univ. Technol., Delft, The Netherlands, Tech. Rep. 20090707, 2009.
- [24] P. V. Mieghem, J. Omic, and R. Kooij, "Virus spread in networks," IEEE/ACM Trans. Netw., vol. 17, no. 1, pp. 1–14, Jun. 2008.
- [25] A. Gray, D. Greenhalgh, L. Hu, X. Mao, and J. Pan, "A stochastic differential equation SIS epidemic model," SIAM J. Appl. Math., vol. 71, no. 3, pp. 876–902, Jan. 2011.
- [26] C. Li, R. van de Bovenkamp, and P. V. Mieghem, "Susceptible-infected-susceptible model: A comparison of N-intertwined and heterogeneous mean-field approximations," *Phys. Rev. E, Stat. Phys. Plasmas Fluids Relat. Interdiscip. Top.*, vol. 86, no. 2, Aug. 2012, Art. no. 026116.
- [27] Y. Wang, Z. Jin, Z. Yang, Z.-K. Zhang, T. Zhou, and G.-Q. Sun, "Global analysis of an SIS model with an infective vector on complex networks," *Nonlinear Anal., Real World Appl.*, vol. 13, pp. 543–557, Apr. 2012.

- [28] D. Guo, S. Trajanovski, R. van de Bovenkamp, H. Wang, and P. Van Mieghem, "Epidemic threshold and topological structure of susceptible-infectious-susceptible epidemics in adaptive networks," *Phys. Rev. E, Stat. Phys. Plasmas Fluids Relat. Interdiscip. Top.*, vol. 88, no. 4, Oct. 2013, Art. no. 042802.
- [29] M. Benaïm and M. W. Hirsch, "Differential and stochastic epidemic models," *Fields Inst. Commun.*, vol. 21, pp. 31–44, Jul. 1999.
- [30] Y. Wang, G. Xiao, and J. Liu, "Dynamics of competing ideas in complex social systems," New J. Phys., vol. 14, no. 1, Jan. 2012, Art. no. 013015.
- [31] P. E. Paré, J. Liu, C. L. Beck, A. Nedić, and T. Başar, "Multi-competitive viruses over static and time-varying networks," in *Proc. IEEE Amer.* Control Conf., Seattle, WA, USA, May 2017, pp. 1685–1690.
- [32] A. Janson, S. Gracy, P. E. Paré, H. Sandberg, and K. H. Johansson, "Analysis of a networked SIS multi-virus model with a shared resource," *IFAC-PapersOnLine*, vol. 53, no. 5, pp. 797–802, Jun. 2020.
- [33] A. Janson, S. Gracy, P. E. Paré, H. Sandberg, and K. H. Johansson, "Networked multi-virus spread with a shared resource: Analysis and mitigation strategies," 2020, arXiv:2011.07569.
- [34] P. E. Paré, J. Liu, C. L. Beck, A. Nedić, and T. Başar, "Multi-competitive viruses over time-varying networks with mutations and human awareness," *Automatica*, vol. 123, Jan. 2021, Art. no. 109330.
- [35] S. Bansal, B. T. Grenfell, and L. A. Meyers, "When individual behaviour matters: Homogeneous and network models in epidemiology," *J. Roy. Soc. Interface*, vol. 4, no. 16, pp. 879–891, Oct. 2007.
- [36] M. E. Hochberg, "Non-linear transmission rates and the dynamics of infectious disease," *J. Theor. Biol.*, vol. 153, no. 3, pp. 301–321, Dec. 1991.
- [37] H. Hu, K. Nigmatulina, and P. Eckhoff, "The scaling of contact rates with population density for the infectious disease models," *Math. Biosci.*, vol. 244, no. 2, pp. 125–134, Aug. 2013.
- [38] N. D. Barlow, "Non-linear transmission and simple models for bovine tuberculosis," *J. Animal Ecol.*, vol. 69, no. 4, pp. 703–713, Jul. 2000.
- [39] C. Gan, X. Yang, W. Liu, Q. Zhu, and X. Zhang, "An epidemic model of computer viruses with vaccination and generalized nonlinear incidence rate," *Appl. Math. Comput.*, vol. 222, pp. 265–274, Oct. 2013.
- [40] W.-M. Liu, H. W. Hethcote, and S. A. Levin, "Dynamical behavior of epidemiological models with nonlinear incidence rates," *J. Math. Biol.*, vol. 25, no. 4, pp. 359–380, 1987.
- [41] L.-X. Yang and X. Yang, "The impact of nonlinear infection rate on the spread of computer virus," *Nonlinear Dyn.*, vol. 82, nos. 1–2, pp. 85–95, Oct. 2015.
- [42] H. Yuan, G. Liu, and G. Chen, "On modeling the crowding and psychological effects in network-virus prevalence with nonlinear epidemic model," *Appl. Math. Comput.*, vol. 219, no. 5, pp. 2387–2397, Nov. 2012.
- [43] S. Ruan and W. Wang, "Dynamical behavior of an epidemic model with a nonlinear incidence rate," *J. Differ. Equ.*, vol. 188, no. 1, pp. 135–163, Feb. 2003.
- [44] H. L. Smith, "Monotone dynamical systems: Reflections on new advances and applications," *Discrete Continuous Dyn. Syst.*, vol. 37, p. 485, Jan. 2017.
- [45] P. D. Leenheer and D. Aeyels, "Stability properties of equilibria of classes of cooperative systems," *IEEE Trans. Autom. Control*, vol. 46, no. 12, pp. 1996–2001, Dec. 2001.
- [46] D. Angeli and E. D. Sontag, "Monotone control systems," *IEEE Trans. Autom. Control*, vol. 48, no. 10, pp. 1684–1698, Oct. 2003.
- [47] V. S. Bokharaie, O. Mason, and M. Verwoerd, "D-stability and delay-independent stability of homogeneous cooperative systems," *IEEE Trans. Autom. Control*, vol. 55, no. 12, pp. 2882–2885, Dec. 2010.
- [48] L. Van Hien and H. Trinh, "Exponential stability of two-dimensional homogeneous monotone systems with bounded directional delays," *IEEE Trans. Autom. Control*, vol. 63, no. 8, pp. 2694–2700, Aug. 2018.
- [49] D. Efimov, T. Raïssi, and A. Zolghadri, "Control of nonlinear and LPV systems: Interval observer-based framework," *IEEE Trans. Autom. Control*, vol. 58, no. 3, pp. 773–778, Mar. 2013.
- [50] F. Forni and R. Sepulchre, "Differentially positive systems," *IEEE Trans. Autom. Control*, vol. 61, no. 2, pp. 346–359, Feb. 2016.
- [51] M. W. Hirsch, "Systems of differential equations which are competitive or cooperative: I. Limit sets," SIAM J. Math. Anal., vol. 13, no. 2, pp. 167–179, Mar. 1982.
- [52] C. Altafini, "Consensus problems on networks with antagonistic interactions," *IEEE Trans. Autom. Control*, vol. 58, no. 4, pp. 935–946, Apr. 2013.

- [53] M. Di Marco, M. Forti, M. Grazzini, and L. Pancioni, "Limit set dichotomy and multistability for a class of cooperative neural networks with delays," *IEEE Trans. Neural Netw. Learn. Syst.*, vol. 23, no. 9, pp. 1473–1485, Sep. 2012.
- [54] M. Ye, B. D. O. Anderson, and J. Liu, "Convergence and equilibria analysis of a networked bivirus epidemic model," 2021, arXiv:2111.07507.
- [55] V. Doshi, S. Mallick, and D. Y. Eun, "Convergence of bi-virus epidemic models with non-linear rates on networks—A monotone dynamical systems approach: Supplementary material," *Commun. Inf. Syst.*, vol. 20, no. 3, pp. 253–281, 2020.
- [56] C. D. Meyer, Matrix Analysis and Applied Linear Algebra, vol. 71. Philadelphia, PA, USA: SIAM, 2000.
- [57] A. Berman and R. J. Plemmons, Nonnegative Matrices in the Mathematical Sciences. Philadelphia, PA, USA: SIAM, 1994.
- [58] J. Yeh, Real Analysis, 2nd ed. Singapore: World Scientific, 2006.
- [59] M. W. Hirsch, "Systems of differential equations that are competitive or cooperative II: Convergence almost everywhere," SIAM J. Math. Anal., vol. 16, no. 3, pp. 423–439, May 1985.
- [60] M. W. Hirsch, "Systems of differential equations which are competitive or cooperative: III. Competing species," *Nonlinearity*, vol. 1, no. 1, pp. 51–71, Feb. 1988.
- [61] M. W. Hirsch, "Systems of differential equations that are competitive or cooperative. IV: Structural stability in three-dimensional systems," SIAM J. Math. Anal., vol. 21, no. 5, pp. 1225–1234, Sep. 1990.
- [62] M. W. Hirsch, "Systems of differential equations that are competitive or cooperative. V. Convergence in 3-dimensional systems," J. Differ. Equ., vol. 80, no. 1, pp. 94–106, Jul. 1989.
- [63] H. L. Smith, "Systems of ordinary differential equations which generate an order preserving flow. A survey of results," SIAM Rev., vol. 30, no. 1, pp. 87–113, Mar. 1988.
- [64] H. L. Smith and H. R. Thieme, "Quasi convergence and stability for strongly order-preserving semiflows," SIAM J. Math. Anal., vol. 21, no. 3, pp. 673–692, May 1990.
- [65] H. L. Smith and H. R. Thieme, "Convergence for strongly order-preserving semiflows," SIAM J. Math. Anal., vol. 22, no. 4, pp. 1081–1101, Jul. 1991.
- [66] M. W. Hirsch and H. L. Smith, "Generic quasi-convergence for strongly order preserving semiflows: A new approach," J. Dyn. Differ. Equ., vol. 16, no. 2, pp. 433–439, Apr. 2004.
- [67] H. L. Smith, Monotone Dynamical Systems: An Introduction to the Theory of Competitive and Cooperative Systems. Washington, DC, USA: American Mathematical Society, 2014.
- [68] (2012). Is My System of ODEs Cooperative? [Online]. Available: https://math.la.asu.edu/~halsmith/identifyMDS.pdf
- [69] U. Krause and P. Ranft, "A limit set trichotomy for monotone nonlinear dynamical systems," *Nonlinear Anal., Theory, Methods Appl.*, vol. 19, no. 4, pp. 375–392, Aug. 1992.
- [70] M. Ye, J. Liu, B. D. O. Anderson, and M. Cao, "Applications of the Poincaré–Hopf theorem: Epidemic models and Lotka–Volterra systems," *IEEE Trans. Autom. Control*, vol. 67, no. 4, pp. 1609–1624, Apr. 2022.
- [71] J. Leskovec and A. Krevl. (Jun. 2014). SNAP Datasets: Stanford Large Network Dataset Collection. [Online]. Available: http://snap.stanford.edu/data
- [72] S. Ross, Stochastic Processes. Hoboken, NJ, USA: Wiley, 1996.
- [73] L. Perko, Differential Equations and Dynamical Systems, 3rd ed. Cham, Switzerland: Springer, 2001.



Vishwaraj Doshi received the B.E. degree in mechanical engineering from the University of Mumbai, Mumbai, Maharashtra, India, in 2015, the master's degree in operations research from North Carolina State University, Raleigh, NC, USA, in 2017, and the Ph.D. degree with the Operations Research Graduate Program from North Carolina State University in 2022. He is currently a part of the Data Science and Advanced Analytics Team, IQVIA. His primary research interests include design of randomized algorithms on graphs and epidemic models on networks.



Shailaja Mallick received the B.Tech. degree in computer science from UCE, Burla, India, and the master's degree in computer systems and networks from the Chalmers University of Technology, Sweden. She is currently pursuing the Ph.D. degree with the Computer Science Department, North Carolina State University. Her current research interests are in the area of social network analysis, network and performance modeling using techniques from mathematical biology, graph theory, stochastic modeling, and simulation.



Do Young Eun (Senior Member, IEEE) received the B.S. and M.S. degrees in electrical engineering from the Korea Advanced Institute of Science and Technology (KAIST), Daejon, South Korea, in 1995 and 1997, respectively, and the Ph.D. degree from Purdue University, West Lafayette, IN, USA, in 2003. Since August 2003, he has been with the Department of Electrical and Computer Engineering, North Carolina State University, Raleigh, NC, USA, where he is currently a Professor. His research interests include distributed optimization

for machine learning, machine learning algorithms for networks, distributed and randomized algorithms for large social networks and wireless networks, epidemic modeling and analysis, and graph analytics and mining techniques with network applications. He has been a member of Technical Program Committee of various conferences, including IEEE INFOCOM, ICC, Globecom, ACM MobiHoc, and ACM Sigmetrics. He is serving on the Editorial Board for IEEE TRANSACTIONS ON NETWORK SCIENCE AND ENGINEERING. Previously, he served for IEEE/ACM TRANSACTIONS ON NETWORKING and Computer Communications journal, and was the TPC Co-Chair of WASA'11. He received the Best Paper Awards in the IEEE ICCCN 2005, IEEE IPCCC 2006, and IEEE NetSciCom 2015, and the National Science Foundation CAREER Award in 2006. He has supervised and coauthored a paper that received the Best Student Paper Award in ACM MobiCom 2007.